

Uncovering Patterns for Adverse Pregnancy Outcomes with Spatial Analysis: Evidence from Philadelphia *

Cecilia Balocchi^{†‡}, Ray Bai^{§¶}, Jessica Liu^{||}, Silvia P. Canelón^{**},
Edward I. George^{||}, Yong Chen^{**}, Mary R. Boland^{**†}

Abstract

In this case study, we analyze the risk of stillbirth and preterm birth in Philadelphia from 2010 to 2017. We exploit a rich electronic health records dataset (45,919 deliveries at hospitals within Penn Medicine), and augmented with neighborhood data from 363 census tracts of Philadelphia. We conduct a two-stage statistical analysis. In the first stage, we introduce a Bayesian spatial logistic regression model to study the *patient-specific* risk of stillbirth and preterm birth. Our model accounts for heterogeneity and spatial autocorrelation between neighborhoods. We find both patient-level characteristics (e.g. self-identified racial/ethnic group) and neighborhood-level characteristics (e.g. violent crime) are highly associated with patient-specific risk of both outcomes. In the second stage, we aggregate the estimates from our spatial model to quantify *neighborhood* risks of stillbirth and preterm birth. We find that neighborhoods in West Philadelphia and North Philadelphia are at highest risk of these outcomes. Specifically, neighborhoods with higher rates of women living in poverty or on public assistance have higher risk, while neighborhoods with higher rates of women who are college-educated or in the labor force have lower risk. Our Bayesian approach provides meaningful uncertainty measures for these neighborhood risk probabilities and would be useful for public health interventions.

1 Introduction

1.1 Background

Although there have been rapid advancements in maternal health over the past several decades, adverse pregnancy outcomes such as stillbirth, preterm birth, neonatal death, post neonatal death, and low birth weight continue to be major public health problems. While there has been a 90 percent reduction in infant mortality over the past century [34], rates of other adverse outcomes such as low birth weight (i.e. birth weight of 2500 grams or less) and stillbirth (i.e. fetal death at or after 20 weeks of pregnancy) have remained largely unchanged [24, 51]. For example, in 2013, a

*Keywords and phrases: conditional autoregressive model, neighborhood analysis, preterm birth, stillbirth, random effects model

[†]School of Mathematics, University of Edinburgh, Edinburgh, United Kingdom

[‡]Co-first author. Email: cecilia.balocchi@ac.ed.uk

[§]Department of Statistics, University of South Carolina, Columbia, SC, USA

[¶]Co-first author. Email: RBAI@mailbox.sc.edu

^{||}The Wharton School, University of Pennsylvania, Philadelphia, PA, USA

^{**}Department of Biostatistics, Epidemiology, and Informatics, University of Pennsylvania, Philadelphia, PA, USA

^{††}Email: bolandm@upenn.edu

total of 23,595 stillbirths were reported in the United States (U.S.) [28]. This represents a country-wide statistic and therefore the number of stillbirths in any individual city for a given year is often very sparse. Preterm birth (i.e. birth before 37 weeks of pregnancy) is another adverse pregnancy outcome that has gradually increased over time, in spite of improved treatments. Preterm birth is far more common than stillbirth. The Centers for Disease Control and Prevention (CDC) estimated that in 2014, preterm birth affected one of every 10 infants in the U.S. [14]. According to the CDC, the U.S. preterm birth rate also rose to 9.93% in 2017, a 1% rise from 2016 (9.85%) and the third straight year of increases in this rate (9.57% in 2014) [32].

Adverse pregnancy outcomes are significantly associated with increased risk of neonatal mortality and morbidity, adverse neuro-developmental and cognitive outcomes, and increased health care costs [40, 59]. To reduce a patient’s likelihood of experiencing an adverse pregnancy outcome, it is crucial to understand the factors that may contribute to them. Gaining insight into these risk factors can help to guide clinical interventions. For example, if an obstetrician knows that a patient’s stillbirth risk is likely to be elevated because of certain preexisting conditions, they can provide targeted clinical care [51]. Such care might entail increased monitoring, more frequent prenatal visits, early induction of labor, or Cesarean deliveries [51]. Understanding patient-specific risk factors can also guide public health policy. For example, it has been estimated that 5.0-7.3 percent of U.S. preterm-related deaths can be attributable to smoking during pregnancy [47]. Based on these estimates, state Medicaid programs have been required to cover tobacco-cessation counseling and drug therapy for pregnant women without cost sharing since 2010 [47].

Apart from *patient-specific* risk, it is also of interest to quantify the *neighborhood* risk of these outcomes. We define a neighborhood as a spatial unit (e.g. a census tract) within a larger geographic area such as a city or a state. The occurrence of adverse perinatal outcomes is often heterogeneous over a large geographic area, with some areas that are more severely affected [49, 60]. Thus, some researchers have argued that it is critical to conduct location-specific analyses in order to better develop targeted intervention strategies for subpopulations at highest risk [49]. With this goal in mind, we estimate the neighborhood risks of stillbirth and preterm birth and study the factors that contribute to neighborhood disparities. While our work is focused on Philadelphia, our methods are generalizable to other cities and localities where neighborhood factors are important.

1.2 Related work and our contributions

The massive growth of electronic health records (EHRs) since the passage of the Health Information Technology for Economic and Clinical Health (HITECH) Act in 2009 has greatly enabled the study of individual (or patient-level) risk factors and facilitated targeted clinical interventions for adverse pregnancy outcomes [38, 35]. Researchers have identified periodontal disease, socioeconomic status, immigration status, family history of low birth weight babies, and preexisting conditions such as diabetes or chronic hypertension as being significantly associated with patient-specific risk for stillbirth or preterm birth [17, 30, 59, 28, 13]. Researchers have also identified environmental (or neighborhood-level) risk factors for patient-specific risk of adverse pregnancy outcomes. Several studies have suggested that neighborhood characteristics such as local exposure to pollutants, residential segregation, crime levels, and income inequality may also contribute to adverse pregnancy outcomes and other maternal outcomes such as severe maternal morbidity [55, 23, 22, 35, 37].

While patient-specific risk of adverse perinatal outcomes has been studied extensively, there has been comparatively less work on quantifying this risk for *geographic areas*. To identify higher-risk regions for preterm birth without relying on predefined geopolitical borders, South et al. [49]

estimated the spatial density of preterm birth probabilities in Hamilton County, Ohio using spatial filtering techniques. Zahrieh et al. [60] and Zahrieh et al. [61] used Bayesian Poisson processes to discover regions with high intensities of stillbirth events in Iowa. While these researchers identified general geographic areas with elevated risk of adverse pregnancy outcomes, they did not quantify the risk of adverse perinatal outcomes for *specific neighborhoods*. In contrast, our motivating dataset (described in Section 2) consists of patients that are nested (and aggregated for privacy reasons) within *predefined* census tracts of Philadelphia. Therefore, we require a multilevel model that explicitly takes this predetermined neighborhood information into account. Further, targeted social policies and programs are often implemented in practice at a neighborhood level [48]. For example, city councils may identify and designate specific neighborhoods as “priority neighborhoods” for targeted investment [48]. For this reason, we aim to quantify the *neighborhood* risks for all the census tracts in Philadelphia.

In this paper, we present a case study on adverse pregnancy outcomes in the city of Philadelphia. Currently the sixth most populous city in the U.S., Philadelphia is a particularly compelling case study because it is a large urban area that has been experiencing population growth and rapid changes to its built environment for the first time in decades [2]. Patient data were obtained from hospitals within the University of Pennsylvania Health System (also known as Penn Medicine) from 2010 to 2017. In addition, spatially varying neighborhood data from the census tracts of Philadelphia were obtained from the U.S. Census Bureau and other government agencies.

Our objective is to study not only patient-specific risk but also *neighborhood risk* for stillbirth and preterm birth in Philadelphia. Recently, there has been growing interest in *place-based* interventions and policies for addressing health disparities [36]. Place-based interventions are approaches for improving population health within a defined geographic location, delivered at a local or regional level rather than at a national level [12, 36]. Our analysis of Philadelphia aims to uncover spatial patterns and to better understand neighborhood disparities for stillbirth and preterm birth. Our findings could potentially help maternal health researchers and practitioners to reduce stillbirth and preterm birth rates at the neighborhood level. In order to disseminate our results to the broader scientific community, we have included a spreadsheet in the online Supplementary Data with the results from our neighborhood risk analysis for all 363 census tracts in our study. We discuss this in more detail in Section 6.

We conduct a two-stage statistical analysis. In the first stage, we introduce a Bayesian conditional autoregressive (CAR) logistic regression model for estimating patient-specific probabilities of stillbirth and preterm birth. Our CAR model accounts for spatial dependence between geographic neighbors and thus facilitates principled sharing of information across different neighborhoods. Moreover, our model is capable of automatically *learning* the amount of spatial autocorrelation from the data. To assess the association of patient-level and neighborhood-level risk factors with patient-specific risks of these outcomes, we also propose to use a measure that we call Bayes- p (originally introduced by Makowski et al. [29] as the Bayesian Probability of Direction). Rather than testing for “significant” or “insignificant” effect sizes, the Bayes- p directly quantifies how well a covariate effect can be distinguished from a null effect.

In the second stage of our analysis, we aggregate the estimates from our spatial model in order to predict the neighborhood probabilities for stillbirth and preterm birth. A key benefit of our Bayesian model is that we can naturally *quantify the uncertainty* of these predicted neighborhood risk probabilities through their posterior distributions. We then cluster the individual census tracts into “lower-risk,” “moderate-risk,” and “higher-risk” neighborhoods for each outcome. This enables

us to identify specific neighborhoods with elevated risk of stillbirth and preterm birth and to quantify the risk disparities between different types of neighborhoods. Finally, we use the clusters that we found to study the factors that contribute to neighborhood disparities.

Our main findings can be summarized as follows. In our first-stage analysis, our CAR model reveals that there is moderate spatial autocorrelation for stillbirth and weak spatial autocorrelation for preterm birth, after accounting for patient-level and neighborhood-level risk factors. Using the Bayes- p measure (described in Section 3), we find that both patient-level and neighborhood-level risk factors are highly associated with patient-specific risk. In particular, patients who self-identify as Black and gave birth to multiple babies are at higher risk of both stillbirth and preterm birth. Higher prevalence of neighborhood violent crime is also associated with increased risk of both outcomes. Moreover, we find that the risk of stillbirth increases for patients living in poorer neighborhoods, while the risk of preterm birth increases for patients in neighborhoods with higher proportions of high school graduates and fewer women participating in the labor force. In our second-stage analysis, we identify the neighborhoods in West and North Philadelphia as being at highest risk for stillbirth and preterm birth. These higher-risk neighborhoods tend to have higher proportions of women living below the poverty line or on public assistance and lower proportions of women who are college-educated or in the labor force.

The rest of the paper is organized as follows. In Section 2, we describe the dataset that motivated our study. In Section 3, we introduce our Bayesian CAR model and the Bayes- p measure for quantifying patient-specific risk factors. In Section 4, we discuss our approaches for quantifying neighborhood risk of adverse pregnancy outcomes. In Section 5, we present the main results from our case study of stillbirth and preterm birth in Philadelphia. Section 6 summarizes our study and discusses the importance and potential impact of our findings.

2 Motivating data

In order to conduct our analysis of stillbirth and preterm birth, we first obtained data on patients who had deliveries at Penn Medicine hospitals from 2010 to 2017. We used a previously developed and validated algorithm by Canelón et al. [8] to identify deliveries from Penn Medicine EHRs. After removing 17,305 observations with either missing values in the patient address or with patients living outside of the city of Philadelphia, our dataset contained an initial total of 46,029 deliveries at Penn Medicine hospitals between 2010 and 2017. Further exclusion criteria for our cohort are described subsequently.

Within each EHR, the following delivery outcomes were annotated: Cesarean section delivery, stillbirth, and preterm birth (each coded as either “1” or “0”). In addition, the EHRs also reported each patient’s residential address, the age of the patient at the time of delivery, binary variables for the patient’s self-reported racial/ethnic group (Hispanic, non-Hispanic White, non-Hispanic Black or non-Hispanic Asian) and a binary variable for multiple birth (e.g. twins, triplets). The vast majority of subjects in our data belonged to only one racial/ethnic group, except for eight patients who identified as belonging to more than one group.

The city of Philadelphia is made up of 384 census tracts determined by the U.S. Census Bureau. We first matched the patients’ residential addresses to their specific longitude and latitude coordinates. Based on these coordinates, we then mapped each of the patients in our dataset to one of 384 census tracts. Because some census tracts were very sparsely populated (e.g. the areas around several rivers, such as the Schuylkill, the Wissahickon and the Pennipack), we removed tracts that

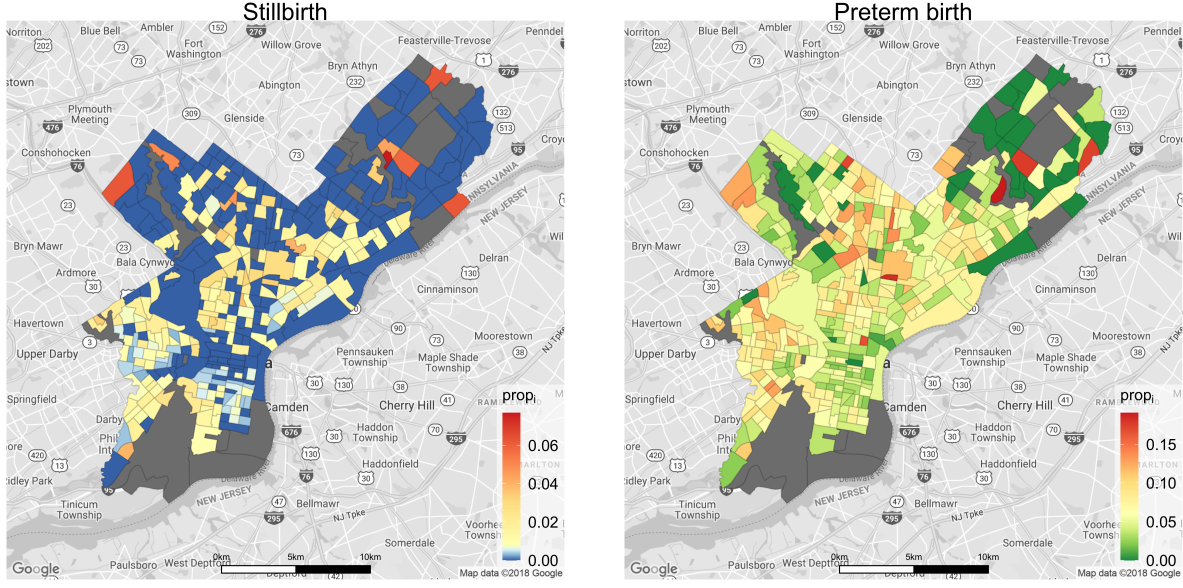


Figure 1: Maps of neighborhood proportions of adverse pregnancy outcomes, either stillbirth (**left panel**) or preterm birth (**right panel**), calculated as the number of adverse outcomes divided by the number of deliveries across all years in each neighborhood. The proportions are displayed only for census tracts included in our study, while regions colored in gray are the census tracts that we excluded from our study.

had fewer than 10 deliveries in each of the eight years. In addition, our CAR model (described in Section 3.1) also requires all geographic areas to be connected, so we also removed neighborhoods that did not share a border with any other tracts with at least 10 deliveries. This preprocessing procedure ultimately removed 21 census tracts and 110 observations from our dataset. Our final cohort contained $N = 45,919$ deliveries in $n = 363$ census tracts, among which had 385 stillbirths and 2897 preterm births. Figure 1 shows the neighborhood proportions of these two adverse pregnancy outcomes after preprocessing. The dark gray tracts are the tracts that were removed from our analysis.

Next, we augmented our dataset with neighborhood covariates based on the census tracts where each of the patients lived. Most of the neighborhood-level data was downloaded in June 2020 from <https://data.census.gov/cedsci/>, the United States Census Bureau’s online data dissemination platform. We downloaded datasets documenting racial makeup, poverty status, education level, and number of housing units for each census tract in Pennsylvania for the years 2010 through 2017. Detailed information on data sources is reported in Section S4 of the Supplementary Material. Intrigued by the possibility that crime could be significantly associated with stillbirth or preterm birth, we also included neighborhood-level data on crime. Our crime data came from <https://opendataphilly.org>, where the Philadelphia Police Department publicly releases the location, time, and type of each reported crime in the city. This crime data was previously analyzed by Balocchi and Jensen [2]. For our study, we included the total number of violent crimes and nonviolent crimes from 2010 to 2017 in each of the census tracts as neighborhood-level predictors. Violent crimes included murders, rapes, robberies and aggravated assaults, whereas nonviolent

Patient-Level	Description
age	Age of the patient
Black	Indicator if the patient self-identifies as Black
Hispanic	Indicator if the patient self-identifies as Hispanic
Asian	Indicator if the patient self-identifies as Asian
multiple birth	Indicator if multiple babies were delivered
Neighborhood-Level	Description
proportion Asian	Proportion of neighborhood that is Asian
proportion Hispanic	Proportion of neighborhood that is Hispanic
proportion Black	Proportion of neighborhood that is Black
proportion women	Proportion of women aged 15-50
poverty	Proportion of women aged 15-50 below the poverty level
public assistance	Proportion of women aged 15-50 who received public assistance
labor force	Proportion of women aged 16-50 who were in the labor force
recent birth	Proportion of women who gave birth in the past 12 months
high school grad	Proportion of women aged 15-50 who graduated high school
college grad	Proportion of women aged 15-50 with a Bachelor’s degree
occupied housing	Total number of occupied housing units (log-transformed)
housing violation	Total number of housing violations (log-transformed)
violent crime	Total number of violent crimes (log-transformed)
nonviolent crime	Total number of nonviolent crimes (log-transformed)

Table 1: The 19 covariates we used in our analysis of adverse pregnancy outcomes in Philadelphia.

crimes included burglaries, larceny/theft, motor vehicle thefts and arson.¹

Table 1 reports all 19 of the patient-level and neighborhood-level covariates that we considered in our study. For the patient-level maternal racial/ethnic group indicator variables in Table 1 (Black, Hispanic, and Asian), the baseline group was White patients. A few of the continuous covariates were heavily skewed right – namely, total number of occupied housing units, total number of housing violations, the total number of violent and nonviolent crimes. Consequently, we considered their log-transformed values. Some additional preprocessing of the data was also done in order to ensure that there was not severe multicollinearity among the covariates. These details are provided in Section S4 of the Supplementary Material.

3 Patient-specific risk analysis

3.1 Bayesian CAR model

Our motivating dataset from Section 2 consists of geospatial data referenced by the census tracts of Philadelphia. In our statistical analysis, we aim to use this neighborhood information. Specif-

¹Our definitions of violent crime and nonviolent crime were based on the designations of offenses by the FBI’s Uniform Crime Reporting Program: <https://ucr.fbi.gov/crime-in-the-u.s/2018/crime-in-the-u.s.-2018/topic-pages/offenses-known-to-law-enforcement> (last accessed June 24, 2022).

ically, we build a model that accounts for both neighborhood heterogeneity *and* potential spatial autocorrelation between neighborhoods.

We propose to use a Bayesian CAR model for modeling adverse pregnancy outcomes, with a prior on the autocorrelation parameter. Let y_{ij} be a binary response variable, with “1” indicating if an adverse pregnancy outcome occurred for delivery j corresponding to a patient living in the i th neighborhood. Suppose that we have n neighborhoods and a total of $N = \sum_{i=1}^n m_i$ observations, where m_i denotes the number of patients in the i th neighborhood. We assume that each y_{ij} follows a conditionally independent Bernoulli distribution, that is,

$$y_{ij} \mid p_{ij} \sim \text{Bernoulli}(p_{ij}), \quad i = 1, \dots, n, j = 1, \dots, m_i. \quad (3.1)$$

A standard model for estimating the p_{ij} ’s in (3.1) is the mixed effects logistic regression model,

$$\log \left(\frac{p_{ij}}{1 - p_{ij}} \right) = \alpha_i + \mathbf{x}_{ij}^\top \boldsymbol{\beta}, \quad (3.2)$$

where \mathbf{x}_{ij} is a p -dimensional vector that contains the p covariates for the patient corresponding to the j th delivery in neighborhood i , $\boldsymbol{\beta} = (\beta_1, \dots, \beta_p)^\top \in \mathbb{R}^p$ is a vector of unknown regression coefficients (the fixed effects), and α_i is a random effect that accounts for the variation in neighborhood i that cannot be explained by the p covariates. We note that in our dataset, the neighborhood covariates in each \mathbf{x}_{ij} in (3.2) also depended on the year in which delivery j in neighborhood i happened. However, we found that the effect of time was fairly negligible, and many of the neighborhood variables did not vary significantly across different years. For notational simplicity, we do not include a subscript for year in (3.1) or (3.2). In Section 6, we discuss how our model can be extended to account for temporal effects.

Let $\boldsymbol{\alpha} = (\alpha_1, \dots, \alpha_n)^\top$ denote the vector of neighborhood-specific random effects. In order to incorporate the neighborhood information in our spatial analysis, we employ a CAR prior on $\boldsymbol{\alpha}$ [4, 26, 27]. The CAR model is a Gaussian Markov random field which induces spatial dependence through an adjacency matrix for the areal units, which in our case study, are the census tracts of Philadelphia. While there are many variations of the CAR prior (see, e.g. Lee [26]), we use the proper CAR formulation of Leroux et al. [27]. Leroux et al. [27] define the distribution of each α_i , given the other entries $\boldsymbol{\alpha}_{-i}$, as a normal distribution centered at a weighted average of a global mean α_0 and the α_j ’s from neighborhoods that share a border with α_i . That is,

$$\alpha_i \mid \boldsymbol{\alpha}_{-i}, \alpha_0, \tau_\alpha^2 \sim \mathcal{N} \left(\frac{\rho \sum_j w_{ij} \alpha_j + (1 - \rho) \alpha_0}{\rho \sum_j w_{ij} + (1 - \rho)}, \frac{\tau_\alpha^2}{\rho \sum_j w_{ij} + (1 - \rho)} \right), \quad (3.3)$$

where the w_{ij} ’s are adjacency weights that are equal to 1 if the neighborhoods i and j share a border and equal to 0 otherwise. The parameter τ_α is a global scale parameter. Meanwhile, $\rho \in [0, 1)$ represents the strength of spatial correlation between the components of $\boldsymbol{\alpha}$, with larger values of ρ corresponding to stronger influence of bordering neighborhoods.

We collect the adjacency weights w_{ij} into an adjacency matrix \mathbf{W} , which we can assume known, because we can easily use the shape files from the U.S. Census Bureau to determine which of the census tracts share a border. As noted in Balocchi and Jensen [2] and proven in Chapter 3 of Banerjee et al. [3], the joint distribution of $\boldsymbol{\alpha}$ is uniquely determined by the set of conditional distributions defined in (3.3) and can be written more compactly as

$$\boldsymbol{\alpha} \mid \alpha_0, \tau_\alpha^2 \sim \mathcal{N} \left(\alpha_0 \cdot \mathbf{1}, \tau_\alpha^2 \boldsymbol{\Sigma}_{\text{CAR}} \right), \quad (3.4)$$

where $\mathbf{1}$ is a n -dimensional vector of all 1's, $\Sigma_{\text{CAR}}^{-1} = \rho(\mathbf{D}_{\mathbf{W}} - \mathbf{W}) + (1 - \rho)\mathbf{I}_n$, and $\mathbf{D}_{\mathbf{W}} - \mathbf{W}$ is the Laplacian matrix based on the neighborhood adjacency matrix \mathbf{W} . Thus, to model the spatial dependence for adverse pregnancy outcomes under model (3.2), we ultimately place the CAR model (3.4) as the prior on $\boldsymbol{\alpha}$.

It should be noted that if $\rho = 0$, then the CAR model (3.4) reduces to a non-spatial multilevel mixed effects model,

$$\boldsymbol{\alpha} \mid \alpha_0, \tau_{\alpha}^2 \sim \mathcal{N}(\alpha_0 \cdot \mathbf{1}, \tau_{\alpha}^2 \mathbf{I}_n). \quad (3.5)$$

The model (3.5) is widely used for modeling multilevel data, and indeed, it is a special case of the CAR model (3.4) where all neighborhoods are assumed to be spatially independent (i.e. $\rho = 0$). There are various hypothesis tests to determine whether a CAR model (3.4) or an independent random effects model (3.5) is appropriate to use. For example, Moran's I statistic [39] has widely been used in practice to test for the presence of significant spatial autocorrelation. As an alternative to testing if $\rho = 0$, a Bayesian approach can be used to adaptively *learn* the amount of spatial autocorrelation from the data and to model the implicit *uncertainty* about ρ . To do this, we endow the spatial autocorrelation parameter ρ in (3.4) with a noninformative uniform prior,

$$\rho \sim \mathcal{U}(0, 1). \quad (3.6)$$

If there is weak or negligible autocorrelation, then the posterior for ρ will concentrate most of its posterior mass near zero. Moreover, since ρ is sampled in each iteration of our Markov chain Monte Carlo (MCMC) algorithm and subsequently used to sample the model parameters $(\boldsymbol{\alpha}, \boldsymbol{\beta})$, we obtain many posterior samples of $(\boldsymbol{\alpha}, \boldsymbol{\beta})$ based on different values of ρ . In this sense, the prior (3.6) also facilitates model averaging over varying degrees of spatial autocorrelation.

To model the uncertainty in the grand mean α_0 in (3.4), we place a relatively noninformative prior on α_0 ,

$$\alpha_0 \sim \mathcal{N}(0, 100). \quad (3.7)$$

We also place a noninformative half-Cauchy prior on the global scale parameter τ_{α} ,

$$\tau_{\alpha} \sim \mathcal{C}^+(0, 1). \quad (3.8)$$

To complete our prior specification, we need to place a prior on the fixed effects $\boldsymbol{\beta}$ in (3.2). To this end, we endow $\boldsymbol{\beta}$ with the prior,

$$\boldsymbol{\beta} \mid \mathbf{b}_0, \tau_{\beta}^2 \sim \mathcal{N}(\mathbf{b}_0, \tau_{\beta}^2 \mathbf{I}_p), \quad (3.9)$$

where we place a relatively noninformative prior on \mathbf{b}_0 ,

$$\mathbf{b}_0 \sim \mathcal{N}(\mathbf{0}_p, 100 \cdot \mathbf{I}_p), \quad (3.10)$$

and a noninformative half-Cauchy prior on the scale τ_{β} ,

$$\tau_{\beta} \sim \mathcal{C}^+(0, 1). \quad (3.11)$$

In short, our Bayesian CAR model can be summarized as follows. We place the hierarchical CAR prior (3.4) with hyperpriors (3.6)-(3.8) on the random effects $\boldsymbol{\alpha}$ and the hierarchical prior (3.9)-(3.11) on the fixed effects $\boldsymbol{\beta}$.

Our model can be implemented using Markov chain Monte Carlo (MCMC). Thanks to the Pólya-Gamma data augmentation strategy of Polson et al. [43], the MCMC updates for $(\boldsymbol{\alpha}, \alpha_0, \boldsymbol{\beta}, \mathbf{b}_0)$ are all available in closed form. Meanwhile, we update $(\tau_{\alpha}, \tau_{\beta}, \rho)$ using adaptive Metropolis-Hastings. Complete details for our MCMC algorithm are provided in Section S5 of the Supplementary Material.

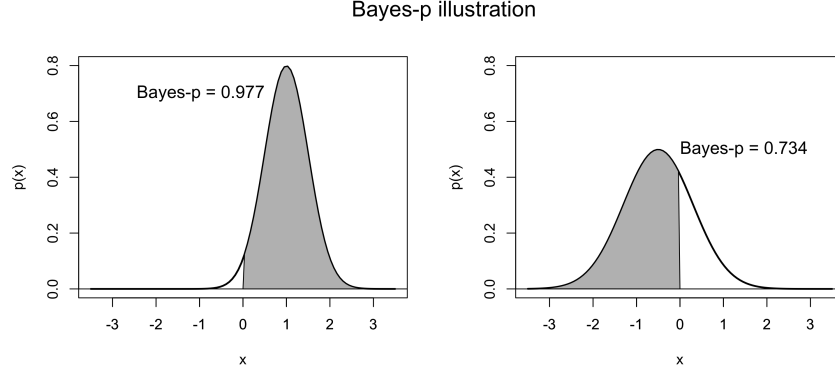


Figure 2: Graphical illustration of the Bayes- p measure, computed on two Gaussian distributions $N(\mu, \sigma^2)$, with the area shaded in gray corresponding to Bayes- p value for each distribution. In the left panel, $\mu = 1, \sigma = 0.5$, and in the right panel, $\mu = -0.5, \sigma = 0.8$.

3.2 The Bayes- p measure

We now describe our inferential approach for quantifying the risk factors for patient-specific risk of stillbirth and preterm birth. In epidemiological studies, it is customary to use either p -values or confidence intervals of the regression coefficients to determine the statistical significance of potential risk factors. However, the final conclusions can be highly sensitive to the choice of p -value significance cutoff or confidence interval percentiles, and it may be preferable to use a quantitative measure for variable association that is more agnostic.

We propose using the Bayes- p measure, also known as the Probability of Direction [29]. The Bayes- p measure for the j th variable is the posterior probability that a coefficient has the sign of its posterior median. The Bayes- p can be computed as the maximum posterior probability that the j th regression coefficient β_j in β is either less than zero or greater than zero. That is,

$$\text{Bayes-}p = \max \{P(\beta_j > 0 \mid \mathbf{y}), P(\beta_j < 0 \mid \mathbf{y})\}. \quad (3.12)$$

Bayes- p (3.12) is a posterior probability quantifying how much of a coefficient’s distribution is non-overlapping with zero. This measures directly how well the effect of a predictor can be distinguished from a null effect. Thus, a higher Bayes- p for a variable indicates that it is more highly associated with the outcome. For example, a predictor whose posterior distribution is centered around zero will be less associated with an outcome than a predictor which has 90% probability of being less than zero. In practice, (3.12) can be calculated using the MCMC samples for each β_j .

It should be stressed that the Bayes- p does not pertain to the hypothesis testing framework and is quite different from a frequentist p -value. The Bayes- p pertains to the amount of posterior probability “away” from zero, while the p -value is the probability of observing values more extreme than a test statistic *under a null hypothesis* $H_0 : \beta_j = 0$. Moreover, while a smaller p -value indicates a higher level of statistical significance, a larger Bayes- p corresponds to predictor that is more highly associated with the outcome.

Figure 2 illustrates two examples of the Bayes- p measure. In the left panel of Figure 2, the 95% credible interval is (0.02, 1.98) (suggesting statistical significance), while the 99% credible interval

is $(-0.29, 2.29)$ (suggesting an *insignificant* association between exposure and outcome). Whereas the choice of $\alpha \in (0, 1)$ in our $100(1 - \alpha)\%$ posterior credible intervals can strongly influence our conclusions, the Bayes- p does not depend on any threshold α . Unlike posterior credible intervals, Bayes- p (3.12) also allows us to directly *compare* the effects of different potential risk factors. In Section 5.2, we illustrate the utility of Bayes- p in our case study on stillbirth and preterm birth in Philadelphia.

4 Neighborhood risk analysis

The approaches that we introduced in Section 3 allow us to quantify the patient-specific risk for stillbirth and preterm birth. However, we are also interested in quantifying the *neighborhood* risk probabilities of these outcomes for each of the $n = 363$ census tracts of Philadelphia. The patient-specific risk analysis in Section 3 is based on conditional comparisons among different risk factors. In other words, the effects of each risk factor are determined *conditionally* on the other covariates in the model. As a result, high correlations between covariates might mask the true association between some of the predictor variables and the outcome of interest. On the other hand, our neighborhood risk analysis allows for *marginal* comparisons of the risk factors between different neighborhoods and clusters of neighborhoods (see Table 3, for example).

First, we define the risk probability p_{ij} for delivery j corresponding to a patient living in the i th census tract as

$$p_{ij} = \frac{e^{\theta_{ij}}}{1 + e^{\theta_{ij}}}, \quad (4.1)$$

where θ_{ij} is the log-odds,

$$\theta_{ij} = \alpha_i + \mathbf{x}_{ij}^\top \boldsymbol{\beta}, \quad (4.2)$$

and α_i and $\boldsymbol{\beta}$ are as in (3.2). Based on all m_i individuals' risk probabilities (4.1) in the i th neighborhood, we define the neighborhood risk probability p_i for the i th neighborhood as

$$p_i = \frac{1}{m_i} \sum_{j=1}^{m_i} p_{ij}. \quad (4.3)$$

Since p_i in (4.3) is a one-to-one function of $(\alpha_i, \boldsymbol{\beta})$, it is straightforward to approximate the posterior distributions of the predicted neighborhood probabilities $p(p_i | \mathbf{y}), i = 1, \dots, n$, using the MCMC samples of $(\boldsymbol{\alpha}, \boldsymbol{\beta})$ from our CAR model in Section 3. This is one of the key benefits of adopting a Bayesian CAR model in our first-stage analysis. We can naturally quantify the *uncertainty* of our predicted neighborhood risk probabilities (4.3) through their posterior distributions in the second stage of our analysis.

In epidemiology, it is common to develop different risk categories for community health. For example, the CDC has categorized all of the U.S. counties' community levels of coronavirus disease 2019 (COVID-19) as either "low," "medium," or "high."² To aid in the interpretability of our results for neighborhood risk of stillbirth and preterm birth, we similarly stratify the census tracts of Philadelphia into three risk categories. Specifically, we take the posterior means \hat{p}_i of $p(p_i | \mathbf{y}), i = 1, \dots, n$ and cluster the predicted \hat{p}_i 's into three groups using k -means clustering: "lower-risk," "moderate-risk," and "higher-risk" neighborhoods. The cluster assignments for the n neighborhoods

²<https://www.cdc.gov/coronavirus/2019-ncov/your-health/covid-by-county.html> (last accessed June 24, 2022)

are then subsequently used to form the aggregate risk posteriors $p(p_{LR} | \mathbf{y})$, $p(p_{MR} | \mathbf{y})$, and $p(p_{HR} | \mathbf{y})$, where p_{LR} , p_{MR} , and p_{HR} denote the predicted probabilities for the lower-risk, moderate-risk, and higher-risk clusters of neighborhoods respectively. For cluster $c \in \{LR, MR, HR\}$, let n_c denote the number of neighborhoods in that cluster. The neighborhood cluster risk is defined as

$$p_c = \frac{1}{n_c} \sum_{i \in c} p_i, \quad (4.4)$$

where p_i is the i th neighborhood’s risk probability (4.3). It is straightforward to obtain the neighborhood cluster risk posterior distributions using the MCMC samples of the p_i ’s. We also use the neighborhood cluster risk probabilities (4.4) to study the discrepancies in neighborhood characteristics between lower-risk, moderate-risk, and higher-risk neighborhoods.

Note that it is possible to stratify the neighborhoods into more than three risk categories. However, for our dataset, we found that the three aggregate risk posterior densities $p(p_{LR} | \mathbf{y})$, $p(p_{MR} | \mathbf{y})$, and $p(p_{HR} | \mathbf{y})$ were fairly well-separated (see Figure 6). Moreover, limiting the number of risk categories to three allowed us to easily detect spatial patterns in neighborhood risk, as we describe in Section 5.3.

5 Results from our case study of Philadelphia

5.1 Model fitting and validation

We now apply the modeling approaches described in Sections 3 and 4 to the study of stillbirths and preterm births in Philadelphia. For the CAR model that we introduced in Section 3, we ran two MCMC chains for a total of 5500 iterations each, using the MCMC algorithm described in Section S5 of the Supplementary Material. For each chain, we removed the first 500 iterations as burn-in. We also thinned our chains every 10 iterations, leaving us with a total of 1000 samples from the two chains. In Section S5 of the Supplementary Material, we also report MCMC diagnostics (trace plots, autocorrelation plots, and MCMC standard errors) to confirm that the number of iterations we used was sufficient to achieve convergence and that our thinned samples were not too correlated. Before fitting our models, we also standardized all the continuous variables to lie on the same scale. Our model’s estimates of the regression coefficients were then transformed back to their original scale for our final analysis.

We used the first six years of data from 2010 to 2016 to perform the patient-specific risk analysis in Section 5.2. The remaining year of data 2017 was used for model validation and for predicting the neighborhood risk probabilities in Section 5.3. We refer to these two datasets as the training set (years 2010 to 2016) and the validation set (year 2017), respectively. The reason that we estimated the neighborhood risk probabilities on a completely out-of-sample validation set was to avoid overfitting. This same approach could be applied to predicting the patient-specific risk probabilities of new patients and deliveries.

5.2 Results for patient-specific risk analysis

We first examined the posterior densities for the autocorrelation parameter ρ under the CAR model fit to the training data. Figure 3 shows the plots of these densities for stillbirth and preterm birth. For stillbirth, we see that the majority of the posterior mass for ρ is between 0.2 and 0.6, with non-negligible mass greater than 0.8. This suggests that the unexplained variation for stillbirth is

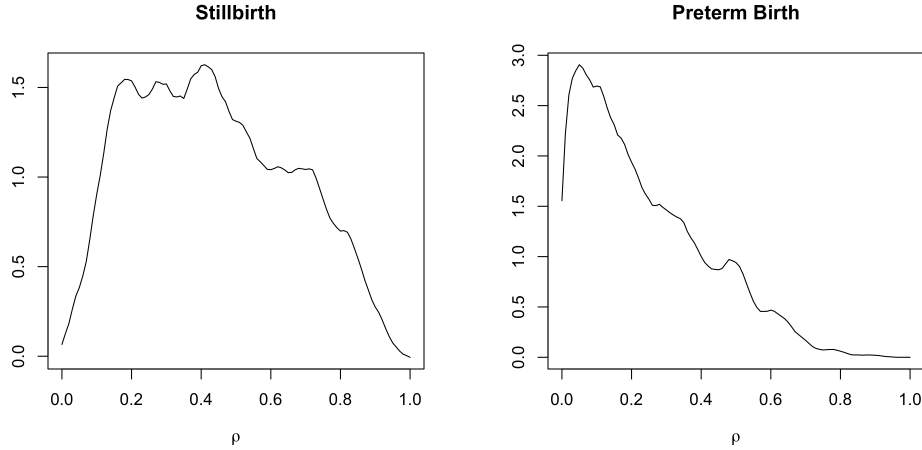


Figure 3: Plots of the posterior densities for autocorrelation parameter ρ for stillbirth (**left panel**) and preterm birth (**right panel**) under the CAR model.

spatially autocorrelated and that some unmeasured, spatially correlated covariates might help to explain the variation in stillbirth. On the other hand, for preterm birth, most of the posterior mass for ρ lies between 0 and 0.2, but there is still some posterior mass on values greater than 0.2. This suggests that there is weaker – but possibly still non-negligible – autocorrelation in the unexplained variation for preterm birth than stillbirth.

To further validate the appropriateness of our spatial model, we also used two different Bayesian information criteria to compare the model fit of the CAR model to a non-spatial Bayesian mixed effects model (i.e. the model (3.2) with (3.5) as the prior on α). These results are reported in Section S1.2 of the Supplementary Material and confirm that the CAR model provides a better fit to our data than a purely non-spatial Bayesian mixed effects model. In Section S3 of the Supplementary Material, we also report comparisons of the CAR model to other non-spatial models.

In Table 2, we report the posterior mean odds ratio (OR) and the Bayes- p (3.12) for all 19 covariates in our CAR model. Recall that the Bayes- p allows for direct comparison of the strength of association between different covariate effects and the outcome of interest, with a larger Bayes- p value indicating a *stronger* association. To visualize these associations, we also plot the 95% posterior credible intervals of the log-odds ratio for these 19 covariates in Figure 4.

We found that self-identifying as Black or Hispanic and experiencing multiple birth were the patient-level risk factors that were the most highly associated with patient-specific risk for stillbirth (Bayes- $p=1$). Among the neighborhood-level risk factors for stillbirth, the proportion of Hispanic and Black residents, the proportion of women living below the poverty line, and the number of both violent and nonviolent crimes were the most highly associated with a patient’s stillbirth risk (Bayes- $p \geq 0.95$). On the other hand, the patient-level risk factors most highly associated with patient-specific risk of *preterm birth* were the patient’s age, whether or not they self-identified as Black, and whether or not they gave multiple birth (Bayes- $p \geq 0.95$). Meanwhile, the neighborhood-level risk factors most highly associated with preterm birth were the number of violent crimes, the neighborhood proportion of Hispanic residents, and the neighborhood proportions of women who were aged 15 to 50, who were in the labor force, or who had graduated high school (Bayes- $p = 1$).

	Stillbirth		Preterm birth	
	OR	Bayes- p	OR	Bayes- p
Patient-level				
age	1.01	0.79	1.00	0.95
Black	2.23	1.00	1.55	1.00
Hispanic	1.61	1.00	0.94	0.79
Asian	0.97	0.58	1.12	0.84
multiple birth	4.17	1.00	10.56	1.00
Neighborhood-level				
proportion Asian	1.01	0.58	0.90	0.58
proportion Hispanic	0.45	0.95	0.72	1.00
proportion Black	0.61	0.95	0.92	0.74
proportion women	0.24	0.89	1.88	1.00
poverty	3.92	1.00	0.87	0.63
public assistance	0.49	0.84	0.89	0.58
labor force	1.25	0.58	0.49	1.00
recent birth	1.40	0.74	1.48	0.79
high school grad	1.16	0.58	2.63	1.00
college grad	0.50	0.89	0.74	0.79
occupied housing	0.99	0.53	0.93	0.68
housing violation	0.88	0.84	0.99	0.68
violent crime	1.59	1.00	1.16	1.00
nonviolent crime	0.75	1.00	0.97	0.63

Table 2: Posterior mean odds ratios (OR) and Bayes- p measures for stillbirth and preterm birth under the CAR model.

We highlight a few specific findings that may warrant further research and action from medical and public health professionals. After controlling for other variables, it appears as though patients who self-identify as Black are at much higher risk of stillbirth (OR=2.23) and preterm birth (OR=1.55), compared to White patients. Self-identified Hispanics are also at much higher risk of stillbirth (OR=1.61) than White patients. Finally, patients experiencing multiple birth are at much higher risk of stillbirth (OR=4.17) and preterm birth (OR=10.56) than those giving birth to only one baby. These findings suggest that both maternal racial/ethnic group and multiple birth play an important role in determining a patient’s likelihood of experiencing stillbirth or preterm birth.

As for neighborhood-level risk factors, we found that after controlling for other variables, an increase in neighborhood violent crime was highly associated with higher risk of both stillbirth (OR=1.59) and preterm birth (OR=1.16). Other than violent crime, increased neighborhood poverty also led to much higher patient-specific risk of stillbirth (OR=3.92), while an increase in proportion of women who graduated from high school led to much higher patient-specific risk of preterm birth (OR=2.63). Finally, an increase in the percentage of women in the labor force was associated with much *lower* patient-specific risk of preterm birth (OR=0.49). These findings suggest that place-based (i.e. targeted) policies and investments to decrease violent crime, alleviate poverty, or increase in the number of women in the labor force may further reduce the patient-specific risk of stillbirth or preterm birth for women living in these neighborhoods.

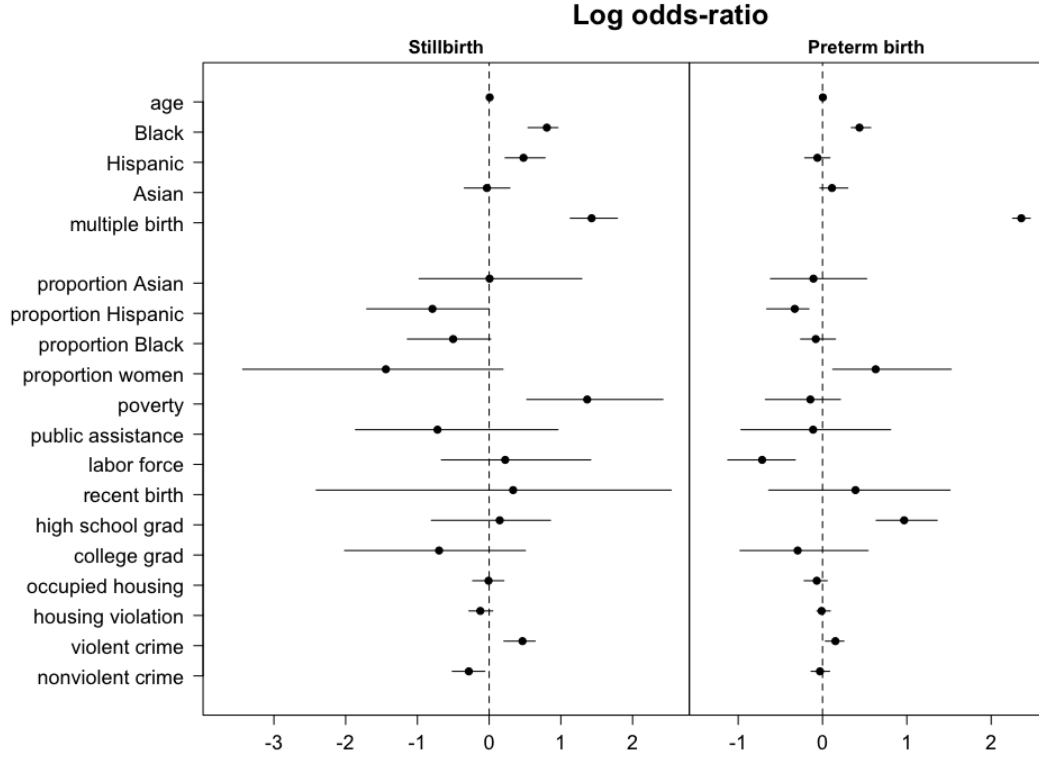


Figure 4: Posterior mean and 95% credible intervals of the log odd-ratios for the 19 covariates under our CAR model. The results are shown for both stillbirth (left) and preterm birth (right).

5.3 Results for neighborhood risk analysis

The top two panels of Figure 5 plot the posterior means of the predicted neighborhood risk probabilities (4.3) for stillbirth and preterm birth. For stillbirth (top left panel of Figure 5), the neighborhoods with the lowest risk probabilities tended to be concentrated in Center City and areas immediately adjacent to Center City (such as Fishtown and Fairmount to the north and Bella Vista and Southwest Center City to the south) and in Northwest Philadelphia. Additionally, some small pockets of census tracts with lower risk can be found in Northeast Philadelphia and West Philadelphia. The census tracts with the highest risk of stillbirth were in North Philadelphia (such as North Philadelphia West), West Philadelphia (such as Cathedral Park, West Parkside, Mantua and Kingsessing) and South Philadelphia (such as Grays Ferry and West Passyunk).

The top right panel of Figure 5 plots the posterior means of the predicted neighborhood probabilities (4.3) for preterm birth. Similar to stillbirth, we found that most of the areas with lower risk of preterm birth were concentrated in Center City and its surrounding neighborhoods and in Northwest Philadelphia, with some small pockets in Northeast Philadelphia and West Philadelphia. Moreover, we also found several census tracts with higher risk of preterm birth in North Philadelphia (especially in North Philadelphia West, Upper North Philadelphia and East Germantown) and in West Philadelphia (especially in Kingsessing, Cathedral Park and West Parkside).

Clustering the neighborhoods into “lower-risk,” “moderate-risk,” or “higher-risk” categories allowed us to more easily visualize the spatial distribution of neighborhood risks for stillbirth and

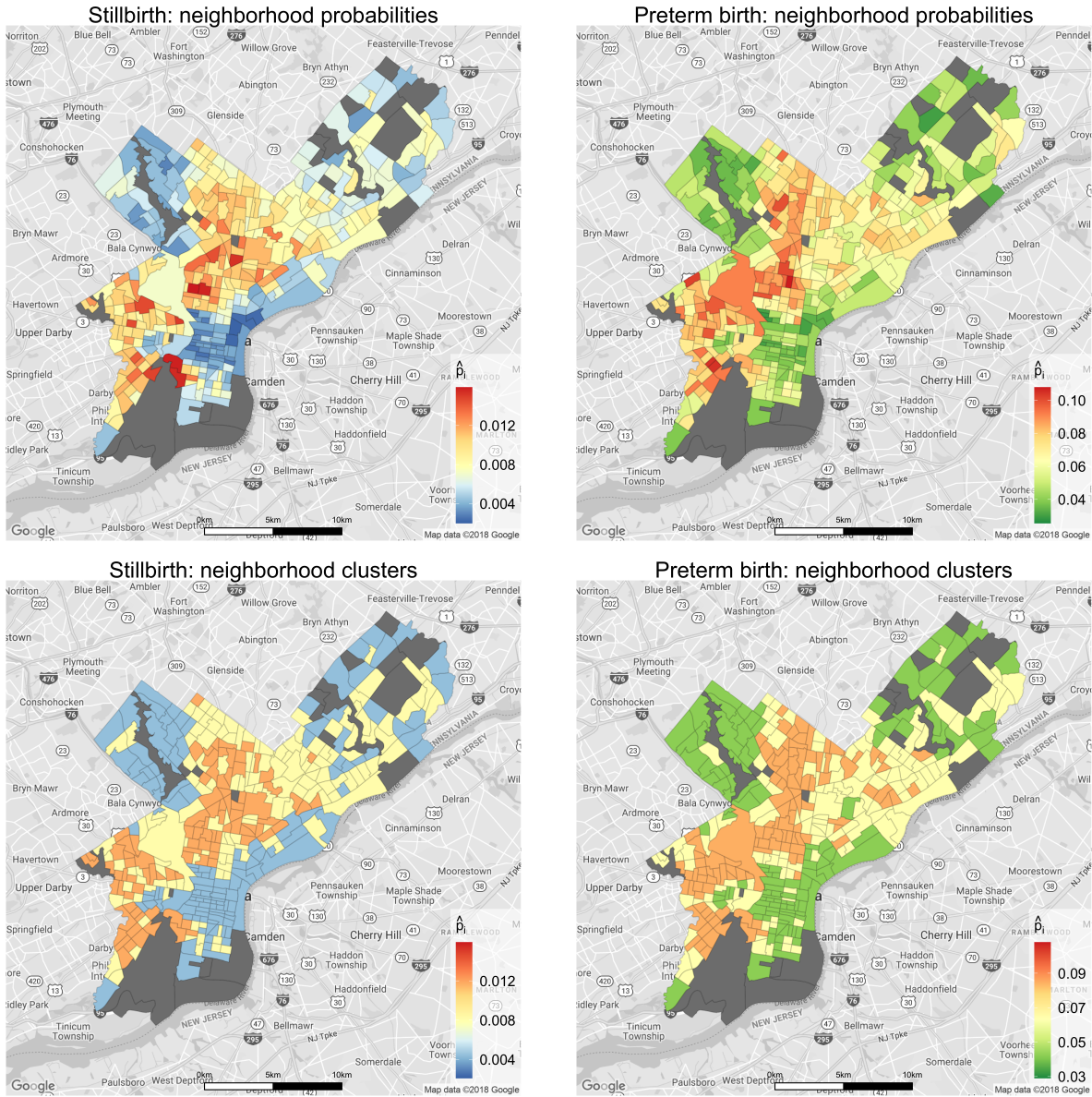


Figure 5: **Top two panels:** Maps of the predicted (posterior mean) neighborhood probabilities of having an adverse pregnancy outcome for stillbirth (left panel) and preterm birth (right panel). **Bottom two panels:** Maps of the clusters of lower-risk, moderate-risk and higher-risk neighborhoods for stillbirth (left panel) and preterm birth (right panel), obtained from running k -means on the predicted neighborhood probabilities.

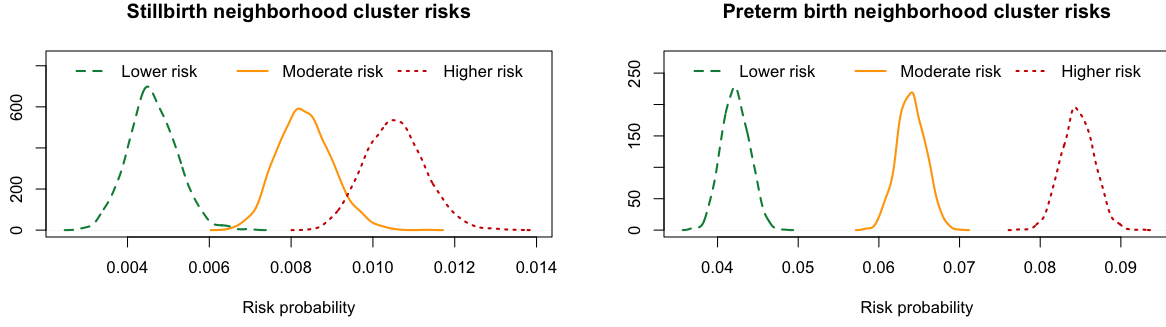


Figure 6: The neighborhood cluster risk posteriors for stillbirth (**left panel**) and preterm birth (**right panel**). The 95% credible intervals for the clusters probabilities are respectively (0.0034, 0.0058), (0.0071, 0.0097) and (0.0092, 0.0120) for stillbirth and (0.039, 0.045), (0.060, 0.067) and (0.081, 0.088) for preterm birth.

preterm birth in Philadelphia. The bottom two panels of Figure 5 plot the cluster assignments for all 363 census tracts. These maps confirm that most of the higher-risk neighborhoods for stillbirth and preterm birth were concentrated in North Philadelphia and West Philadelphia. In addition, North Philadelphia and Northeast Philadelphia also contained many moderate-risk clusters. Table 3 shows the number of neighborhoods in each risk category. In particular, 95 neighborhoods were categorized as “higher-risk” for stillbirth, and 112 neighborhoods were categorized as “higher-risk” for preterm birth.

Figure 6 plots the neighborhood cluster risk posterior distributions $p(p_{LR} | \mathbf{y})$, $p(p_{MR} | \mathbf{y})$, and $p(p_{HR} | \mathbf{y})$ for the three risk categories. We see that the cluster risks (4.4) for the higher-risk group were on average *more than double* those for the lower-risk group. In particular, the posterior mean risks for the higher-risk neighborhoods were 0.0118 for stillbirth and 0.0847 for preterm birth. For lower-risk neighborhoods, the posterior mean risks dropped to 0.0044 for stillbirth and 0.0422 for preterm birth. Moreover, there was no overlap between the 95% credible intervals for $p(p_{LR} | \mathbf{y})$ and $p(p_{MR} | \mathbf{y})$ for either stillbirth or preterm birth. This suggests that our model was able to separate the neighborhoods with elevated (moderate or higher) risk of stillbirth and preterm birth. The results from our neighborhood risk stratification could be useful for planning targeted neighborhood interventions.

Previous research has found that neighborhoods in North and West Philadelphia tend to have poorer health outcomes than other neighborhoods in Philadelphia and the city as a whole. For example, the Philadelphia Department of Health and the Dornsife School of Public Health at Drexel University have found that residents in North and West Philadelphia are burdened with lower lifespans on average and higher rates of high cholesterol, hypertension, diabetes, and heart disease than Philadelphia as a whole. This data was obtained from the Philadelphia Health Rankings website, <https://phillyhealthrankings.org/>. Our findings on the elevated neighborhood risk of stillbirth and preterm birth in North and West Philadelphia seem to be consistent with previous findings on other poor health outcomes in these same neighborhoods. We note that the website Philadelphia Health Rankings has not tracked the neighborhood incidences for either stillbirth or preterm birth. Based on our findings, we believe that these adverse pregnancy outcomes should also be monitored closely by public health practitioners in Philadelphia.

	Stillbirth				Preterm birth			
	Lower risk	Moderate risk	Higher risk	Up/down	Lower risk	Moderate risk	Higher risk	Up/down
\hat{p}_c	0.44%	0.81%	1.18%		4.22%	6.40%	8.47%	
n_c	126	142	95		119	132	112	
proportion Asian	0.09	0.07	0.03	–	0.09	0.07	0.03	–
proportion Hispanic	0.07	0.14	0.14	+	0.08	0.18	0.08	
proportion Black	0.16	0.50	0.78	+	0.16	0.43	0.80	+
proportion women	0.30	0.28	0.28	–	0.29	0.28	0.29	
poverty	0.17	0.28	0.41	+	0.17	0.29	0.37	+
public assistance	0.03	0.08	0.11	+	0.03	0.07	0.12	+
labor force	0.77	0.68	0.63	–	0.77	0.68	0.64	–
recent birth	0.04	0.05	0.06	+	0.04	0.06	0.06	+
high school grad	0.17	0.30	0.35	+	0.16	0.30	0.35	+
college grad	0.29	0.13	0.07	–	0.31	0.13	0.07	–
occupied housing	7.26	7.28	7.31		7.31	7.29	7.24	
housing violation	3.87	4.45	5.00	+	3.75	4.51	4.93	+
violent crime	3.91	4.54	5.08	+	3.81	4.62	4.97	+
nonviolent crime	4.64	4.54	4.73		4.52	4.68	4.67	+

Table 3: Predicted (posterior mean) neighborhood cluster risk probability (\hat{p}_c), number of neighborhoods (n_c), and average neighborhood characteristics for the clusters of lower, moderate and higher-risk neighborhoods. Plus and minus signs indicate the direction of each of the neighborhood characteristics (i.e. whether they tend to increase or decrease with higher risk), if they are determined to be significantly different from zero.

Finally, we used our predicted cluster risk probabilities to study the discrepancies in neighborhood characteristics. For each of the neighborhood-level covariates in Table 1, we computed the mean covariate value within each cluster and regressed these on the clusters’ risk probabilities. Table 3 summarizes our main results. The “Up/down” column in Table 3 indicates the sign of the slope of the regression if the slope was found to be significantly different from zero. More detailed results from this analysis are given in Section S1.2 of the Supplementary Material.

From Table 3, we see that neighborhoods with higher risk of stillbirth and preterm birth tended to have higher proportions of Black residents, higher proportions of women living below the poverty line and on public assistance, and higher numbers of housing violations and violent crimes. On the other hand, neighborhoods with lower risk of these outcomes also tended to have higher proportions of Asian residents and higher proportions of women who were in the labor force or who had graduated from college. Our findings suggest that place-based policies to reduce poverty and violent crime may be beneficial in reducing the neighborhood risk of stillbirth and preterm birth. In addition, expanding educational opportunities and labor force participation among women may also lower the neighborhood risk of stillbirth and preterm birth.

While we have done a comparative study of different clusters of neighborhoods in this section, our model also facilitates comparisons between specific individual neighborhoods that may be of interest. In Section S1.3 of the Supplementary Material, we present pairwise neighborhood risk comparisons for four representative pairs of neighborhoods. These pairs of neighborhoods have very different values for at least one of the covariates in Table 3. For example, in one of the pairs, the first neighborhood has a very low proportion of college-educated women (≈ 0.00), while the second

neighborhood has a fairly high proportion of college-educated women (0.71). The posterior mean risk for stillbirth in the first neighborhood is about 3.7 times that for the second neighborhood. It is interesting to see how the neighborhood risk changes between individual neighborhoods that have very different neighborhood characteristics. Comparisons between more than two neighborhoods can also be similarly done.

6 Discussion

In this paper, we have presented a case study on stillbirth and preterm birth in Philadelphia. We used a rich EHR dataset of 45,919 deliveries at Penn Medicine hospitals from 2010 to 2017, augmented with spatially varying neighborhood data from the U.S. Census Bureau and other government agencies. We analyzed both the patient-specific and neighborhood risk of these adverse pregnancy outcomes. To model the patient-specific risk, we employed a Bayesian CAR model, which accounts for neighborhood heterogeneity and automatically learns the amount of spatial autocorrelation between neighborhoods from the data. Instead of assessing statistical significance using posterior credible intervals, we also used the Bayes- p measure (3.12) to assess how well the effects of different risk factors could be distinguished from a null effect. To model the neighborhood risk, we aggregated the estimates from our CAR model to estimate and quantify the uncertainty of the predicted risk probabilities for both individual neighborhoods and clusters of neighborhoods.

6.1 Importance and potential impact of our findings

In this case study, we found that both patient-level and neighborhood-level risk factors were highly associated with patient-specific risk of stillbirth and preterm birth (see Table 2). In particular, maternal racial/ethnic group and multiple birth were found to be highly associated with increased risk of both of these outcomes. These results may be useful for developing patient-specific clinical interventions for higher-risk patients [51]. Previous research has linked neighborhood exposure to violent crime and “small for gestational age” infants, with the key finding being that across all racial/ethnic groups, there was a negative association between economic disadvantage and birth weight [33]. Our findings support this prior work while building upon it. Namely, we found that neighborhood-level violent crime was *also* highly associated with increased risk of two other important maternal health outcomes: stillbirth and preterm birth. Moreover, our results confirm previous research findings on the relationship between poverty and higher risk of stillbirth [19]. These results could potentially guide public policies to reduce neighborhood stressors that may be triggering these adverse fetal outcomes.

Going further than patient-level risk, our models have also enabled the development of measures of *neighborhood* risk assessment. We are able to group neighborhoods into lower, moderate, and higher risk for stillbirth and preterm birth and provide meaningful uncertainty measures for these clusters’ risk probabilities (see Figure 6). These neighborhood assignments can help in the identification of place-based public health interventions to target communities that may have lower access to health care for a variety of reasons.

In order to aid maternal health researchers and practitioners, we have included a spreadsheet in the online Supplementary Data to disseminate the results from our neighborhood risk analysis. For each of the 363 census tracts in our study, this spreadsheet lists the neighborhood risk category (“lower-risk”, “moderate-risk”, or “higher-risk”), the predicted (posterior mean) neighborhood risk

probability (4.3), and the 95% credible intervals for the neighborhood risk probability for both stillbirth and preterm birth.

Our model detected a clear spatial pattern for neighborhood risk of stillbirth and preterm in Philadelphia. Neighborhoods in West Philadelphia and North Philadelphia were identified as being at highest risk for preterm birth and stillbirth (see Figure 5). In particular, our analysis revealed that higher-risk neighborhoods tended to have lower rates of women who had completed a college education or who were in the labor force. Higher-risk neighborhoods also tended to have higher rates of women who were living below the poverty line or who were on public assistance (see Table 3). Since we assessed the *marginal* comparisons of the risk factors in our neighborhood risk analysis, this seemingly contradictory result is explained by the collinearity between poverty and public assistance. However, when we inspect the effect of public assistance in the *joint* (and conditional) analysis that models patient-specific risk (see Table 2), we find that conditional on poverty, public assistance does not seem to have an effect on the risk for stillbirth or preterm birth. These findings are important, especially since some prior work found a protective effect of public assistance against COVID-19 in the city of Philadelphia [7], while our findings suggest that public assistance may not have a similar protective effect against stillbirth or preterm birth. On the other hand, improved access to educational and employment opportunities might reduce the risk of these outcomes. Overall, this underscores the importance of studying neighborhood-level factors and their contributions to specific health outcomes of interest, since the relationships between neighborhood characteristics and health outcome risks may vary depending on the outcome.

6.2 Other considerations about the data and the model

One particular challenge with our dataset is that stillbirth and preterm birth are rare events, with stillbirth accounting for 0.84% of all 45,919 deliveries in our dataset and preterm birth accounting for 6.3% of all deliveries. In Section S2 of the Supplementary Material, we explore the use of data rebalancing and reweighting methods to mitigate the low incidence of stillbirth and preterm births in our data. Unfortunately, these methods did not significantly improve upon our original model’s predictive performance. We believe that higher-resolution covariates than the ones that were available to us may be needed to greatly improve the predictive performance of our CAR model.

The final models in our study did not account for temporal variation across our eight years of data. In preliminary analysis, we included a random effect for time in our model, so our model was

$$y_{itj} \sim \text{Bernoulli}(p_{itj}), \quad \log \left(\frac{p_{itj}}{1 - p_{itj}} \right) = \alpha_i + \gamma_t + \mathbf{x}_{itj}^\top \boldsymbol{\beta}, \quad (6.1)$$

where the additional subscript t indexes the year in which delivery j in neighborhood i happened. However, we found that the effect of time was fairly negligible and that including a temporal random effect did not improve our model fit. This was likely because many of the covariates (such as the proportions of different racial/ethnic groups or educational attainment) did not vary significantly within neighborhoods across years. However, if there is reason to believe that the temporal effect is significant, we could extend the model introduced in Section 3 to explicitly account for temporal variation by using the model (6.1) and placing independent normal priors on the γ_t ’s in (6.1). Another option for accounting for temporal variation is to employ the semiparametric (or partially linear) mixed model framework where time is included as a covariate and its effect is modeled

nonparametrically. Letting t_{ij} be the year that delivery j in neighborhood i happened, the partially linear model is

$$y_{ij} \sim \text{Bernoulli}(p_{ij}), \quad \log \left(\frac{p_{ij}}{1 - p_{ij}} \right) = \alpha_i + \mathbf{x}_{ij}^\top \boldsymbol{\beta} + f(t_{ij}). \quad (6.2)$$

In addition to placing priors on $(\boldsymbol{\alpha}, \boldsymbol{\beta})$ under (6.2), we could also place a Gaussian process prior on the function $f(\mathbf{t}) = (f(t_{11}), \dots, f(t_{1m_1}), \dots, f(t_{n1}), \dots, f(t_{nm_n}))^\top$. We could also approximate $f(t_{ij})$ as a linear combination of d B-spline basis functions, i.e. $f(t_{ij}) \approx \sum_{k=1}^d \gamma_k B_k(t_{ij})$, and place independent priors on the basis coefficients $\gamma_1, \dots, \gamma_d$.

Acknowledgments

We are grateful to the anonymous reviewers, the Editor, and the Associate Editor, whose thoughtful comments and suggestions helped to greatly improve this paper. This work was initiated when the first listed author was a PhD student at the Wharton School, University of Pennsylvania, under the mentorship of the fifth listed author and the second listed author was a postdoc at the Perelman School of Medicine, University of Pennsylvania, under the mentorship of the sixth and seventh listed authors. We would also like to thank Phiwinhlanhla Ndebele-Ngwenya for her early work on a summer project (mentored by Dr. Boland) involving zip code level analysis that helped to motivate this expanded work.

Funding

The first listed author was supported by the European Research Council (ERC) under the European Union’s Horizon 2020 research and innovation programme under grant agreement No. 817257. The second listed author was partially supported by generous funding from the College of Arts and Sciences at the University of South Carolina and NSF grants OIA-1655740 and DMS-2015528. The fourth and seventh listed authors were supported by generous funding from the University of Pennsylvania Perelman School of Medicine and NIH NCATS grant UL1-TR001878. The fifth listed author was supported by NSF grant DMS-1916245. The sixth listed author was supported by NIH grants 1R01AI130460 and 1R01LM012607.

Software and data availability

All methods were implemented in the statistical environment R [44], using packages [43, 16, 11, 42, 6, 57, 58, 20, 5, 45, 46, 52, 54]. Due to patient privacy concerns, we do not have permission to release or make the Penn Medicine data publicly available. However, code to implement our models and simulated synthetic data to run these scripts are available at <https://github.com/cecilia-balocchi/geospatial-adverse-pregnancy>.

Supplementary Materials for “Uncovering Patterns for Adverse Pregnancy Outcomes with Spatial Analysis: Evidence from Philadelphia”

S1 Additional results for the CAR model

S1.1 Assessing the appropriateness of a spatial model

In Section 3.1 of the main manuscript, we argued that employing a CAR model (3.4) with a uniform prior (3.6) on the autocorrelation parameter ρ allowed us to adaptively learn the degree of spatial autocorrelation between neighborhoods and model the implicit uncertainty in ρ . This makes it a potentially more appealing than simply employing a Bayesian mixed effects model with independent random effects (3.5) for the neighborhoods.

Figure 3 of the main manuscript suggested that there was moderate spatial autocorrelation for stillbirth and weak spatial autocorrelation for preterm birth. To further investigate the appropriateness of a CAR model for our data, we also compared the fit of our CAR model (3.4) to a Bayesian model with independent random effects (3.5) (i.e. ρ fixed *a priori* as $\rho = 0$). We compared these two models on the real dataset (described in Section 2 of the main manuscript) using two separate Bayesian model selection criteria: the Deviance Information Criterion (DIC) [50] and the Watanabe-Akaike information criterion (WAIC) [56].

For an unknown parameter θ , the deviance is $D(\theta) = -2 \log p(\mathbf{y}|\theta)$, where $p(\mathbf{y}|\theta)$ is the likelihood for the respective model. The DIC is given by $D(\bar{\theta}) + 2p_D$ where the first term is the deviance evaluated at the posterior mean of θ , and $p_D = \bar{D}(\bar{\theta}) - D(\bar{\theta})$ is the effective number of model parameters where $\bar{D}(\bar{\theta}) = E_{\theta|\mathbf{y}}[D(\theta)]$ is the posterior mean deviance. The DIC rewards better fitting models through the first term and penalizes more complex models through the second term. The model with the smallest overall DIC value is preferred. As an alternative to DIC, one can also consider the WAIC. The WAIC is given by $\text{WAIC} = -2 \log \bar{p}(\mathbf{y}|\bar{\theta}) + 2p_W$ where $\bar{p}(\mathbf{y}|\bar{\theta})$ is the posterior predictive density of the observed data, and $p_W = \sum_{i,j} \text{Var}[\log p(y_{ij}|\theta)|\mathbf{y}]$, as recommended in [15]. Compared to DIC, WAIC considers the predictive density averaged over the posterior distribution, instead of conditioning on a point estimate, resulting in an approach more in line with the Bayesian framework.

Let $\theta = (\alpha, \beta)$. In our present framework with the mixed effects logistic regression model (3.2), the likelihood is defined as $p(\mathbf{y}|\theta) = \prod_{i,j} p(y_{ij}|\theta) = \prod_{i,j} [p_{ij}(\theta)^{y_{ij}} (1 - p_{ij}(\theta))^{1-y_{ij}}]$, where $p_{ij}(\theta) = \exp(\alpha_i + \mathbf{x}_{ij}^\top \beta) / (\exp(\alpha_i + \mathbf{x}_{ij}^\top \beta) + 1)$. In practice, we estimate $\bar{\theta}$, $\bar{D}(\bar{\theta})$, $\bar{p}(\mathbf{y}|\bar{\theta})$ and $\text{Var}[\log p(y_{ij}|\theta)|\mathbf{y}]$ using MCMC samples from the algorithm described in Section S5 and then compute the DIC as

$$\text{DIC} = 2\bar{D}(\bar{\theta}) - D(\bar{\theta}) \quad (\text{S1})$$

and WAIC as

$$\text{WAIC} = -2 \log \bar{p}(\mathbf{y}|\bar{\theta}) + 2 \sum_{i,j} \text{Var}[\log p(y_{ij}|\theta)|\mathbf{y}]. \quad (\text{S2})$$

The model with the smallest DIC or WAIC provides the best model fit.

We fit the CAR and the independent random effects (indRE) to our training set and computed the DIC (S1) and WAIC (S2) using the validation set. The training and validation data are described in Section 5.1 of the main manuscript. Our results are presented in Table S1. We see that the CAR model has a smaller DIC and WAIC for both stillbirth and preterm birth. This suggests that the CAR model is more appropriate to use than the indRE model for this particular dataset. However, we reiterate that by putting a prior on ρ as in (3.6), we are capturing the *inherent* uncertainty in the spatial autocorrelation ρ . Therefore, we believe that the CAR model is still appropriate to use for areal data even when spatial autocorrelation is fairly negligible. In this case, the CAR model would still be able to adaptively learn the absence of strong autocorrelation, and the posterior mass for ρ would be concentrated near zero.

	Stillbirth		Preterm birth	
	CAR	indRE	CAR	indRE
DIC	380.1	382.3	883.8	885.1
WAIC	380.3	382.5	883.8	885.2

Table S1: Comparisons of model fit for the CAR model vs. the independent random effects model using DIC and WAIC.

S1.2 Additional results for the neighborhood risk analysis

In Section 5.3 of the main manuscript, we presented a comparative analysis of the neighborhood characteristics between “lower-risk,” “moderate-risk,” and “higher-risk” clusters of neighborhoods that we found. Here, we regressed the mean neighborhood covariate values of each cluster on the posterior mean predicted risk probabilities for each cluster. The main results of this analysis were reported in Table 3 of the main manuscript. In Tables S2 and S3, we report more detailed results for stillbirth and preterm birth respectively. In the rightmost columns of Tables S2 and S3, we report the magnitudes of the estimated slope and the p-values from the simple linear regression models that we fit.

In addition to these simple linear regressions, we also performed one-way analysis of variance (ANOVA) tests to test whether the mean neighborhood covariate values differed significantly across lower-risk, moderate-risk, and higher-risk groups of neighborhoods. We report the F -statistics and p-values from these ANOVA tests in the second rightmost columns of Tables S2 and S3. We see that there is agreement between the ANOVA tests and the linear regression models that we fit. Namely, if the ANOVA test determined that there was no significant difference between the lower-risk, moderate-risk, and higher-risk groups for a particular neighborhood characteristic (occupied housing and nonviolent crime for stillbirth; and proportion women, occupied housing, and housing violations for preterm birth), then the linear regression slope for that neighborhood characteristic was also *not* significantly different from zero.

Stillbirth	Lower risk	Moderate risk	Higher risk	ANOVA		Slopes	
\hat{p}	0.44%	0.81%	1.18%				
	\bar{x}_j	\bar{x}_j	\bar{x}_j	F-value	p-value	β	p-value
proportion Asian	0.0862	0.0673	0.0266	16.3005	0.0000	-7.9247	0.0000
proportion Hispanic	0.0729	0.1441	0.1367	6.3663	0.0019	9.2469	0.0042
proportion Black	0.1606	0.5012	0.7776	144.7190	0.0000	84.1930	0.0000
proportion women	0.2974	0.2808	0.2762	5.0093	0.0071	-2.9566	0.0030
poverty	0.1659	0.2828	0.4120	102.9180	0.0000	33.2907	0.0000
public assistance	0.0328	0.0824	0.1130	58.5833	0.0000	11.0247	0.0000
labor force	0.7675	0.6820	0.6320	48.3316	0.0000	-18.6495	0.0000
recent birth	0.0394	0.0546	0.0617	18.8219	0.0000	3.0859	0.0000
high school grad	0.1690	0.3006	0.3521	110.1243	0.0000	25.4390	0.0000
college grad	0.2945	0.1303	0.0699	195.1799	0.0000	-31.2494	0.0000
occupied housing	7.2564	7.2836	7.3087	0.4074	0.6657	7.1142	0.3668
housing violation	3.8695	4.4477	5.0005	52.0092	0.0000	153.6266	0.0000
violent crime	3.9053	4.5420	5.0788	95.5258	0.0000	159.9585	0.0000
nonviolent crime	4.6378	4.5386	4.7254	3.0265	0.0497	9.7213	0.3644

Table S2: Average neighborhood characteristics of the clusters of lower-risk, moderate-risk, and higher-risk neighborhoods for **stillbirth**; results from three-way ANOVA tests, and results from simple linear regression on the cluster risk probabilities.

Preterm	Lower risk	Moderate risk	Higher risk	ANOVA		Slopes	
\hat{p}	4.22%	6.40%	8.47%				
	\bar{x}_j	\bar{x}_j	\bar{x}_j	F-value	p-value	β	p-value
proportion Asian	0.0870	0.0694	0.0306	15.8705	0.0000	-1.3188	0.0000
proportion Hispanic	0.0802	0.1794	0.0840	13.6561	0.0000	0.1865	0.7340
proportion Black	0.1603	0.4263	0.8029	184.8069	0.0000	15.0807	0.0000
proportion women	0.2904	0.2794	0.2870	1.3702	0.2554	-0.0905	0.5923
poverty	0.1671	0.2935	0.3712	67.5253	0.0000	4.8321	0.0000
public assistance	0.0309	0.0749	0.1163	70.4655	0.0000	2.0140	0.0000
labor force	0.7705	0.6797	0.6444	44.4952	0.0000	-2.9971	0.0000
recent birth	0.0412	0.0556	0.0567	10.8672	0.0000	0.3721	0.0000
high school grad	0.1561	0.2999	0.3505	141.7264	0.0000	4.6243	0.0000
college grad	0.3080	0.1338	0.0709	257.6153	0.0000	-5.6392	0.0000
occupied housing	7.3053	7.2916	7.2418	0.6980	0.4982	-1.4778	0.2668
housing violation	3.7539	4.5071	4.9331	65.1284	0.0000	27.9321	0.0000
violent crime	3.8085	4.6217	4.9665	108.7947	0.0000	27.5036	0.0000
nonviolent crime	4.5159	4.6786	4.6676	2.9690	0.0526	3.6579	0.0428

Table S3: Average neighborhood characteristics of the clusters of lower-risk, moderate-risk, and higher-risk neighborhoods for **preterm birth**; results from three-way ANOVA tests, and results from simple linear regression on the cluster risk probabilities.

S1.3 Pairwise comparisons of neighborhood risks

In Section 5.3 of the main manuscript, we provided a visualization of the posterior mean predicted probabilities of an adverse outcome for each neighborhood (Figure 5 of the main manuscript). However, to better compare how the collective set of covariates affects the neighborhood risk, we compare several pairs of neighborhoods which differ for one or more neighborhood-level covariates.

So far, we have presented results in terms of the odds ratio (OR) for each predictor, but this can be misleading since the covariates cannot be artificially changed keeping the others fixed. Thus, we now study how neighborhood-level covariates jointly change by considering four representative pairs of neighborhoods.

It is important not to consider the predictors in isolation (as they are often correlated), but to analyze the differences between two neighborhoods for all their covariates jointly. For a given predictor of interest, consider a pair of neighborhoods that display the minimum and maximum values for such predictors. One can then visualize how the other covariates change and how all of them affect the change in neighborhood risk of an adverse pregnancy outcome.

Table S4 reports the comparisons for four representative pairs of neighborhoods, displaying their covariates and the neighborhood OR for an adverse pregnancy outcome. The i th neighborhood's OR can be computed as $\exp(\theta_i)$, where θ_i is the neighborhood log-odds ratio as in (4.2). These pairs of neighborhoods were chosen to maximize the discrepancy in the proportion of Black inhabitants (B_{\min} and B_{\max}), the proportion of women in the labor force (L_{\min} and L_{\max}), the proportion of women who graduated from college (C_{\min} and C_{\max}) and the level of violent crime (V_{\min} and V_{\max}).

It is interesting to notice that the pairs of neighborhoods do not differ only in the level of the chosen predictor. For example, B_{\min} and B_{\max} have very different proportions of women who are college graduates. L_{\min} and L_{\max} also differ in the proportion of women below the poverty line, while V_{\min} and V_{\max} have very different levels of housing violations. The last four rows of the table compare the predicted risk of stillbirth and preterm birth for each pair of neighborhoods, along with the fraction of the two odds ratios.

	B_{\min}	B_{\max}	L_{\min}	L_{\max}	C_{\min}	C_{\max}	V_{\min}	V_{\max}
Stillbirth								
\hat{p}	0.38%	1.1%	0.71%	0.22%	1.41%	0.38%	0.29%	0.92%
OR ₂ /OR ₁	291.67%		31.4%		26.76%		321.1%	
Preterm birth								
\hat{p}	3.44%	8.49%	9.15%	4.52%	7.56%	3.44%	3.4%	8.03%
OR ₂ /OR ₁	260.71%		47.04%		43.51%		247.85%	
proportion Asian	0.11	0.00	0.43	0.04	0.01	0.09	0.01	0.02
proportion Hispanic	0.01	0.00	0.02	0.06	0.00	0.12	0.04	0.18
proportion Black	0.00	1.00	0.17	0.07	0.98	0.02	0.00	0.63
proportion women	0.39	0.23	0.59	0.36	0.25	0.30	0.20	0.31
poverty	0.23	0.32	0.95	0.08	0.48	0.22	0.00	0.35
public assistance	0.01	0.12	0.00	0.00	0.02	0.01	0.00	0.19
labor force	0.78	0.54	0.12	0.98	0.60	0.75	0.63	0.68
recent birth	0.01	0.02	0.00	0.00	0.07	0.09	0.07	0.06
high school grad	0.00	0.17	0.03	0.02	0.29	0.00	0.04	0.39
college grad	0.56	0.03	0.03	0.54	0.00	0.71	0.38	0.03
occupied housing	7.64	6.99	5.33	7.62	7.44	7.72	6.21	7.84
housing violation	3.56	5.21	1.82	4.09	5.36	4.45	0.48	5.93
violent crime	4.43	4.82	4.57	4.63	5.05	4.44	0.48	6.23
nonviolent crime	5.66	4.17	5.63	5.77	5.04	5.65	3.14	5.74

Table S4: Comparison of risk probabilities and relative odds ratio for pairs of neighborhoods that differ for a specific neighborhood level characteristic: “proportion Black” for neighborhoods B_{\min} and B_{\max} , “labor force” for neighborhoods L_{\min} and L_{\max} , “college grad” for neighborhoods C_{\min} and C_{\max} , and “violent crime” for neighborhoods V_{\min} and V_{\max} .

S1.4 Spatial distribution of estimated random effects

In Figure S1, we plot the posterior means $\hat{\alpha}_i$ ’s of the neighborhood random effects for the 363 census tracts in our CAR model. Recall that the random effect α_i in (3.2) accounts for the variation in risk for neighborhood i that cannot be explained by the fixed covariates \mathbf{x}_{ij} . Figures 5 and 6 of the main manuscript are a bit easier to interpret than Figure S1, since Figures 5 and 6 depict the predicted neighborhood risk probabilities of adverse pregnancy outcomes. However, we include Figure S1 here for the sake of completeness.

S2 Data rebalancing and data reweighting

One potential challenge with our dataset is that stillbirth and preterm birth are rare events. The incidence of stillbirth accounts for 0.84% (385 stillbirths) of all 45,919 deliveries, while preterm birth accounts for 6.3% of all deliveries (2897 preterm births). Thus, it is possible that we have an underrepresented sample of stillbirths and preterm births. This scenario is also known as an *imbalanced* dataset.

Let $y_i \in \{0, 1\}$ be a binary variable for the i th observation, where “1” indicates a positive case and “0” indicates a negative case (or a control). Define $p_i = P(y_i = 1 \mid \mathbf{x}_i)$, where $\mathbf{x}_i :=$

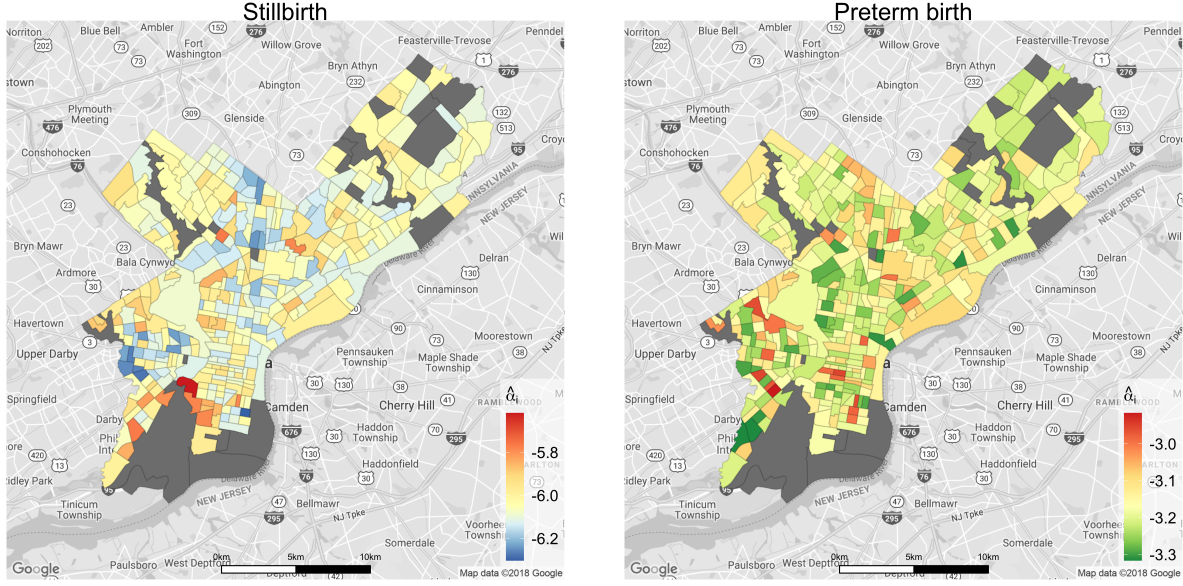


Figure S1: Maps of the posterior means of the neighborhood random effects α_i from the CAR model. **Left panel:** Results for stillbirth. **Right panel:** Results for preterm birth.

$(1, x_{i1}, \dots, x_{ip})^\top \in \mathbb{R}^{p+1}$ is a vector of p covariates, augmented with a one for the intercept. A standard logistic regression model is $p_i = \exp(\mathbf{x}_i^\top \boldsymbol{\beta}) / (1 + \exp(\mathbf{x}_i^\top \boldsymbol{\beta}))$, $i = 1, \dots, n$, where $\boldsymbol{\beta} := (\beta_0, \beta_1, \dots, \beta_p) \in \mathbb{R}^{p+1}$ is the vector of regression coefficients. King and Zeng [21] and Manski and Lerman [31] have shown that for logistic regression with rare events, the estimated probabilities \hat{p}_i may be underestimated for the true cases ($y_i = 1$) when the sample cases are underrepresented. As a result, logistic regression may have poor discriminative ability for the true cases when the sample contains much fewer cases than controls.

In the literature, there are two major ways to deal with this issue: data rebalancing and data reweighting. Data rebalancing creates a balanced dataset by randomly removing (i.e. undersampling) controls or oversampling cases *before* fitting the model. See Chapter 16 of Kuhn and Johnson [25]. A particularly popular balancing method is the Synthetic Minority Over-sampling Technique (SMOTE) [9]. SMOTE creates new synthetic cases by using a random sample and its k -nearest neighbors in the covariate space. For each continuous covariate, SMOTE randomly finds two nearest neighbors in the minority class, produces a new point midway between the two existing points, and adds that new covariate value to the dataset. For binary or categorical data, the SMOTE method takes the most commonly occurring category of nearest neighbors to create new covariate values [53]. Meanwhile, SMOTE also simultaneously undersamples the majority class until the number of cases and controls is roughly the same. After SMOTE rebalancing, a statistical model can then be fit to the rebalanced dataset. In a variety of applications, SMOTE has been shown to improve predictive power, sometimes drastically [9, 62].

Another common approach for mitigating imbalanced data is to reweight the cases and controls. For parametric models, this would entail assigning weights to the individual terms in the likelihood

[31, 21]. For logistic regression, the reweighted likelihood can be expressed as

$$L_w(\boldsymbol{\beta} \mid \mathbf{y}) = \prod_{i=1}^n \left(\frac{\exp(y_i \mathbf{x}_i^\top \boldsymbol{\beta})}{1 + \exp(\mathbf{x}_i^\top \boldsymbol{\beta})} \right)^{w_i}, \quad (\text{S1})$$

where w_i is a weight assigned to the i th observation. For imbalanced data, we would typically assign greater weight to the cases than the controls [18]. Manski and Lerman [31] and King and Zeng [21] proposed choosing the weights as $w_1 = \tau/\bar{y}$ for the cases ($y_i = 1$) and $w_0 = (1 - \tau)/(1 - \bar{y})$ for the controls ($y_i = 0$), where τ is the fraction of cases in the population and \bar{y} is the fraction of cases in the sample. Manski and Lerman [31] showed that this weighted maximum likelihood estimator (MLE) $\hat{\boldsymbol{\beta}}$ for (S1) is a consistent and asymptotically normal estimator, provided that the probability of cases in the population τ is known. In practice, if τ is unknown, then it is common to instead assign a weight of $w_1 = 1$ for the cases and $w_0 = n_1/n_0$ for the controls in (S1), where n_1 is the number of cases and n_0 is the number of controls [18]. This has the effect of *downweighting* the controls, which can improve logistic regression’s discriminative ability for the rare cases.

S2.1 CAR-SMOTE and CAR-Reweight

Since our dataset was imbalanced for both outcomes, with much fewer cases than controls, we explored the use of SMOTE and likelihood reweighting for the CAR model introduced in Section 3 of the main manuscript. In this section, we describe the methods that we used to employ these approaches with our data, which we denote as CAR-SMOTE and CAR-Reweight respectively.

We first describe the CAR-SMOTE procedure. Recall that SMOTE creates synthetic cases to artificially balance the data. The main challenge with deploying SMOTE in our particular context is that we want to preserve the neighborhood information from the U.S. Census Bureau when we create new cases of the rare event. That is, we do *not* want to create new neighborhood-level covariates; instead, we want to use the same neighborhood values as those reported by the U.S. Census for each census tract. Accordingly, we used *only* the patient-level covariates in Table 1 of the main manuscript, as well as the year of delivery and the longitude and latitude coordinates of the addresses for the N original subjects to create synthetic data. The new SMOTE-generated longitude and latitude coordinates were then matched to their census tracts, and the neighborhood covariate values for those tracts were augmented to the synthetic data. After balancing the dataset using SMOTE, we then fit the CAR model to the rebalanced data.

For the CAR-Reweight model, we used a reweighted likelihood

$$L_w(\boldsymbol{\alpha}, \boldsymbol{\beta} \mid \mathbf{y}) = \prod_{i=1}^n \prod_{j=1}^{m_i} \left(\frac{\exp(y_{ij}(\alpha_i + \mathbf{x}_{ij}^\top \boldsymbol{\beta}))}{1 + \exp(\alpha_i + \mathbf{x}_{ij}^\top \boldsymbol{\beta})} \right)^{w_i}, \quad (\text{S2})$$

in place of the usual mixed effects logistic regression likelihood (i.e. (S2) with $w_{ij} = 1$ for all $i = 1, \dots, n, j = 1, \dots, m_i$). We endowed the parameters $(\boldsymbol{\alpha}, \boldsymbol{\beta})$ with the same hierarchical priors $p(\boldsymbol{\alpha})$ and $p(\boldsymbol{\beta})$ as those used in Section 3 of the main manuscript. Bayesian inference was then carried out as

$$p_w(\boldsymbol{\alpha}, \boldsymbol{\beta} \mid \mathbf{y}) \propto L_w(\boldsymbol{\alpha}, \boldsymbol{\beta} \mid \mathbf{y}) p(\boldsymbol{\alpha}) p(\boldsymbol{\beta}). \quad (\text{S3})$$

In line with common practice [18], we assigned a weight of $w_1 = 1$ for all of the cases and $w_0 = n_1/n_0$ for all of the controls in (S2), where n_1 is the number of adverse pregnancy outcomes and n_0 is the

Method	Stillbirth	Preterm Birth
CAR	0.667	0.709
CAR-SMOTE	0.532	0.569
CAR-Reweight	0.681	0.707

Table S5: Comparison of the AUC for CAR, CAR-SMOTE, and CAR-Reweight.

number of controls. That is, we *downweighted* the controls in the CAR-Reweight model. Thanks to the Pólya-Gamma data augmentation algorithm of Polson et al. [43], we could still easily use MCMC to obtain the posterior samples of (α, β) for the reweighted model (S3).

S2.2 Results

Here, we present results for CAR-SMOTE and CAR-Reweight, compared to the original CAR model introduced in Section 3 of the main manuscript. Similarly as in Section 5 of the main manuscript, we fit these models on the training set. We then used the parameter estimates from our training set to predict the patient-specific probabilities of stillbirth or preterm birth for the deliveries in the *validation set*. We computed the area under the curve (AUC) of the receive-operator curve for CAR, CAR-SMOTE, and CAR-Reweight. The AUC comparisons for CAR, CAR-SMOTE, and CAR-Reweight are given in Table S5. Note that a higher AUC indicates better predictive accuracy. In addition to comparing the predictive performance, we also compared the 95% posterior credible intervals for the different risk factors. These results are depicted in Figures S2 (for CAR-SMOTE) and S3 (for CAR-Reweight).

We note that the main motivation for using SMOTE and reweighting is often to improve *predictive performance*. Unfortunately, as shown in Table S5, using SMOTE with our CAR model resulted in much worse out-of-sample AUC for both stillbirth (AUC=0.532) and preterm birth (AUC=0.569) than the original CAR models (AUC=0.667 for stillbirth and AUC=0.709 for preterm birth). Therefore, we do not recommend using SMOTE with the CAR model for the Philadelphia dataset. On the other hand, using a reweighted likelihood for our CAR model provided a slight improvement in AUC for stillbirth (AUC=0.681). For preterm birth, there was a slight decrease in AUC for the CAR-Reweight model (AUC=0.707) from the original CAR model. Overall, the performance of the reweighted CAR model seemed to be similar to the original CAR model.

Based on Figures S2 and S3, we can see that many of the posterior mean effect sizes were similar under CAR-SMOTE and CAR-Reweight as the original CAR model. However, Figure S2 shows that there were a few covariates where the mean effect size changed drastically both in terms of the sign and magnitude under CAR-SMOTE. In addition, as shown in Figure S3, many of the credible intervals were much wider and more of them contained zero under the CAR-Reweight model. This also resulted in most of the Bayes- p values becoming smaller under CAR-Reweight than the Bayes- p under the original CAR model. Thus, CAR-Reweight was not able to pick up on as many signals as the original CAR model. Both these behaviors were also confirmed in a small simulation study ran with synthetic data similar to the real data (results not shown).

Given these differences from the original CAR model, we caution against the use of SMOTE and likelihood reweighting for statistical inference. SMOTE and reweighting are primarily used when *prediction* is the primary objective, rather than inference. As shown in Figures S2 and S3, inference with SMOTE and reweighting may differ quite a bit from the original model. In our case study, we

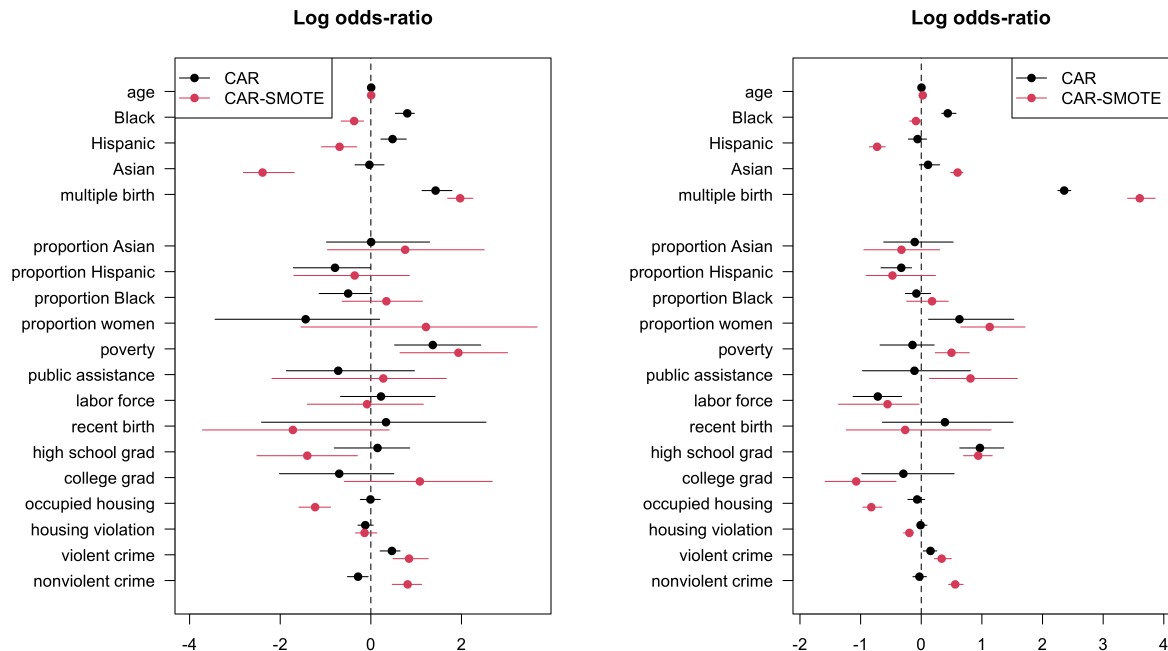


Figure S2: Posterior mean and 95% credible intervals of the log odd-ratios for the CAR and CAR-SMOTE methods. **Left panel:** Results for stillbirth. **Right panel:** Results for preterm birth.

are not only interested in prediction of stillbirth or preterm birth risk; we are *also* concerned with performing valid inference of the patient-level and neighborhood-level risk factors for these adverse pregnancy outcomes. For this reason, we presented only the results for the *original* CAR model in the main manuscript.

S3 Comparison to frequentist models

In this section, we compare our Bayesian CAR model with other frequentist models. Specifically, we compared our model's performance to:

- regular logistic regression (GLM)
- mixed effects logistic regression with a random effect for neighborhood (GLMM)
- random forest (RF).

We also considered SMOTE versions of the above models (GLM-SMOTE), (GLMM-SMOTE), RF-SMOTE. In this case, we applied SMOTE rebalancing to the dataset (as described in Section S2) before fitting the respective GLM, GLMM, and RF models. We also considered data reweighting methods. For GLM and GLMM, we downweighted the controls in the likelihood function by a factor of n_1/n_0 , similarly as did for the CAR model in Section S2. We refer to these approaches as GLM-Reweight and GLMM-Reweight. For random forests, we considered two approaches for imbalanced data introduced by Chen et al. [10]: *balanced* random forest (BRF) and *weighted* random forest

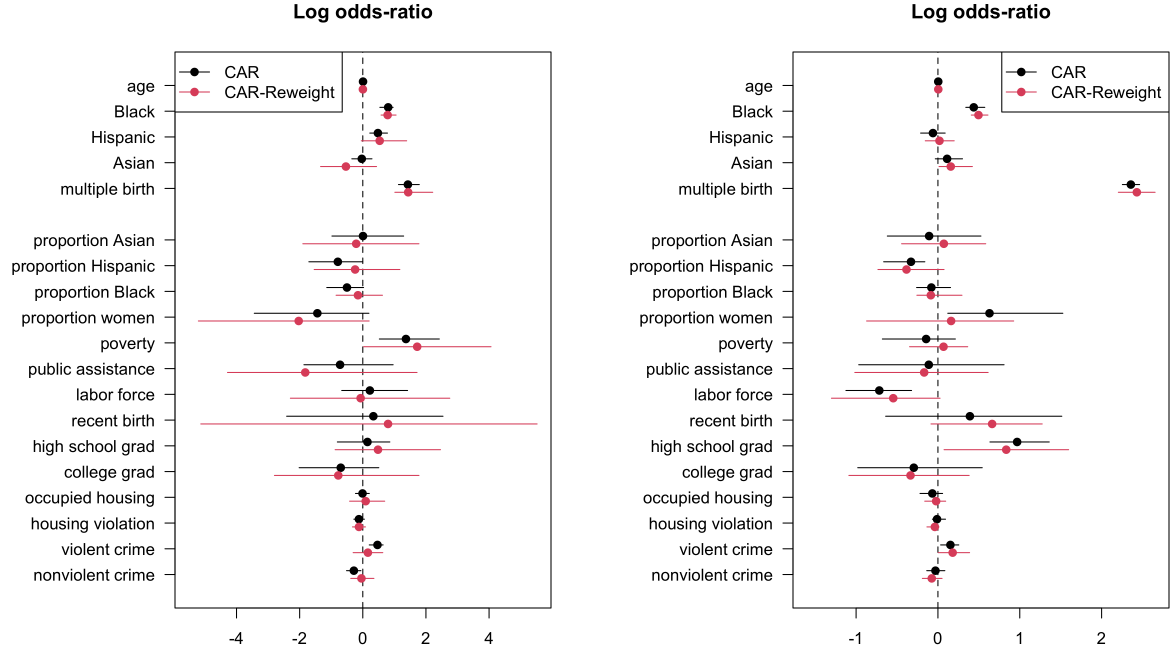


Figure S3: Posterior means and 95% credible intervals of the log odd-ratios for the CAR and CAR-Reweight methods. **Left panel:** Results for stillbirth. **Right panel:** Results for preterm birth.

(WRF). In BRF, the individual decision trees are required to be balanced in the sense that each tree is constructed from a bootstrap sample containing an equal number of cases as controls. In WRF, class weights are assigned to each class, similarly as for GLM-Reweight and GLMM-Reweight. However, in WRF, the class weights are used to reweight the Gini criterion for finding splits and to reweight the votes from individual trees for determining the final ensemble classifications. More details for BRF and WRF are given in Chen et al. [10]. Similar to GLM-Reweight and GLMM-Reweight, we assigned a weight of one to the cases and downweighted the controls in WRF by a factor of n_1/n_0 .

We fit all of the models on the training set and used the estimates to compute the out-of-sample AUC for the validation set. In Table S6, we report the AUC for the original CAR, CAR-SMOTE, and CAR-Reweight models, compared against these frequentist approaches. We see from Table S6 that on this particular dataset, SMOTE and data reweighting did not seem to dramatically improve the predictive accuracy of the original models. Moreover, despite being ostensibly more flexible, the RF approaches performed worse than the parametric models.

For stillbirth, the CAR-Reweight model had the highest AUC of 0.681 out of all the models. Among the original *non*-rebalanced and *non*-reweighted approaches (i.e. CAR, GLM, GLMM, and RF), the CAR model also had the highest AUC of 0.667. Based on this, the spatial CAR model seems to be the most appropriate in terms of prediction. This is consistent with our findings in the left panel of Figure 3 in the main manuscript, which demonstrated that there was moderate spatial autocorrelation for stillbirth. For preterm birth, the regular non-Bayesian GLMM had the highest AUC of 0.715, but this was not much higher than the CAR model's AUC of 0.709. Recall

Method	Stillbirth	Preterm Birth
CAR	0.667	0.709
GLM	0.663	0.713
GLMM	0.656	0.715
RF	0.619	0.644
CAR-SMOTE	0.532	0.569
GLM-SMOTE	0.648	0.704
GLMM-SMOTE	0.595	0.713
RF-SMOTE	0.614	0.684
CAR-Reweight	0.681	0.707
GLM-Reweight	0.671	0.715
GLMM-Reweight	0.510	0.664
BRF	0.604	0.687
WRF	0.582	0.639

Table S6: Comparison of the AUC for the CAR models vs. the frequentist models.

that by the right panel of Figure 3 of the main manuscript, most of the posterior mass for the autocorrelation parameter ρ was concentrated near zero. This figure suggests that there is weak spatial autocorrelation for preterm birth. Therefore, the spatial model and the non-spatial models may be expected to perform similarly in the case of preterm birth.

Despite having somewhat similar predictive performance to the frequentist approaches, we argue that the Bayesian model that we proposed in Section 3 of the main manuscript has several benefits over non-Bayesian approaches:

1. It can adaptively learn the amount of spatial autocorrelation $\rho \in [0, 1)$ from the data and model the inherent uncertainty in ρ through a prior distribution on ρ .
2. It allows us to directly quantify how well a covariate’s effect can be distinguished from a null effect through the Bayes- p measure (3.12).
3. It provides principled uncertainty quantification for both the effect sizes of the regression coefficients *and* the predicted neighborhood risk probabilities through their posterior densities.

S4 Additional data information

In Section 2 of the main manuscript, we described the data used for our analysis of adverse pregnancy outcomes in Philadelphia. While the patient-level data from Penn Medicine EHRs is not publicly available, the neighborhood-level data were downloaded from <https://data.census.gov/cedsci/> and from <https://opendataphilly.org>. In Table S7, we describe the precise data source for each covariate. In addition, we describe some additional preprocessing of the dataset below.

In our dataset of $N = 45,919$ deliveries, we initially included an indicator variable for whether the patient self-identified as White (**White**) and the neighborhood proportion of those identifying as White (**proportion White**) as covariates in our model. However, when we included both of these covariates, the variance inflation factors (VIF) for **White** and **proportion White** were greater than 9.5. The VIF was also greater than 9.5 for the individual and neighborhood-level race factors in

Neighborhood-level covariate	Source	Data File
Proportion of each census tract that identifies as Asian Alone	ACS	B01001D
Proportion of each census tract that identifies as Black or African-American	ACS	B01001B
Proportion of each census tract that identifies as Hispanic or Latinx	ACS	B01001I
Proportion of each census tract that identifies as White Alone	ACS	B01001A
Proportion of women aged 15-50 years in each census tract	ACS	S1301
Proportion of women aged 15-50 years in each census tract below 100 percent poverty level	ACS	S1301
Proportion of women aged 15-50 years in each census tract that received public assistance income in the past 12 months	ACS	S1301
Proportion of women aged 16-50 years in each census tract that are in the labor force	ACS	S1301
Proportion of women aged 15-50 years in each census tract who had a birth in the past 12 months	ACS	B13016
Proportion of women aged 15-50 years in each census tract that graduated high school (including equivalency)	ACS	S1301
Proportion of women aged 15-50 years in each census tract that have a Bachelor's degree	ACS	S1301
Number of occupied housing units in each census tract	ACS	S2502
Housing Violations	OpenDataPhilly	
Violent Crime Rate	OpenDataPhilly	
Non-Violent Crime Rate	OpenDataPhilly	

Table S7: Sources and data files for neighborhood-level covariates used in our analysis. ACS refers to the American Community Survey

Table 1 of the main manuscript (i.e. `Black`, `Hispanic`, `Asian`, `proportion Asian`, `proportion Hispanic`, and `proportion Black`), indicating the presence of significant multicollinearity among all of the race variables [41]. The reason for this was because in the majority of cases, we could deduce the values for `White` and `proportion White` if the other variables were known. For example, if we observed `Black = Hispanic = Asian = 0`, then the patient typically identified as `White` (i.e. `White = 1`). On the other hand, if one of the non-White patient-level race variables in Table 1 of the main manuscript was equal to one, then we could infer that typically the patient's individual race was not `White` (i.e. `White=0`).

The neighborhood proportion of White residents could also often be determined by taking $\text{proportion White} \approx 1 - (\text{proportion Asian} + \text{proportion Hispanic} + \text{proportion Black})$, since the proportions of Philadelphia residents identifying as Native American, Pacific Islander, Alaskan Native or Native Hawaiian were very small and therefore excluded from our analyses. Once we removed the variables `White` and `proportion White`, the VIFs for all patient-level and neighborhood-level covariates were below 9.5, indicating much less severe multicollinearity among the remaining covariates.

S5 Computational details and MCMC diagnostics

S5.1 MCMC algorithm

To fit our CAR model in Section 3.1 of the main manuscript, we sample from the posterior distribution with MCMC. We use a Gibbs sampler to iteratively sample from the full conditional posteriors, together with the data augmentation strategy using Pólya-Gamma latent variables, proposed by

Polson et al. [43]. This strategy is the equivalent in logistic regression to the data augmentation strategy using latent Gaussian random variables in probit regression [1].

Using the notation from Polson et al. [43], we say that a random variable X is distributed from a Pólya-Gamma with parameters $b > 0$ and $c \in \mathcal{R}$ if

$$X \stackrel{D}{=} \frac{1}{2\pi^2} \sum_{k=1}^{\infty} \frac{g_k}{(k - 1/2)^2 + c^2/(4\pi^2)},$$

where $g_k \sim \text{Ga}(b, 1)$, and we denote $X \sim PG(b, c)$.

As shown in Polson et al. [43], if $y_i \sim \text{Bernoulli}(\pi_i)$ and $\log(\frac{\pi_i}{1-\pi_i}) = \mathbf{x}_i^\top \boldsymbol{\beta}$ with $\boldsymbol{\beta} \sim \mathcal{N}(\mathbf{b}, \mathbf{B})$, we can sample

$$\begin{aligned} \omega_i | \boldsymbol{\beta} &\sim PG(1, \mathbf{x}_i^\top \boldsymbol{\beta}), \\ \boldsymbol{\beta} | \mathbf{y}, \boldsymbol{\omega} &\sim \mathcal{N}(\mathbf{m}_\omega, \mathbf{V}_\omega), \end{aligned}$$

with $\mathbf{V}_\omega = (\mathbf{X}^\top \boldsymbol{\Omega} \mathbf{X} + \mathbf{B}^{-1})^{-1}$ and $\mathbf{m}_\omega = \mathbf{V}_\omega (\mathbf{X}^\top \boldsymbol{\Omega} \tilde{\mathbf{y}} + \mathbf{B}^{-1} \mathbf{b})$, where $\boldsymbol{\Omega} = \text{diag}(\omega_i)$ and $\tilde{y}_i = \frac{y_i - \frac{1}{2}}{\omega_i}$.

To adapt this sampling scheme to our model, we can write $\alpha_i + \mathbf{x}_{ij}^\top \boldsymbol{\beta} = \mathbf{z}_{ij}^\top \boldsymbol{\alpha} + \mathbf{x}_{ij}^\top \boldsymbol{\beta}$, where \mathbf{z}_{ij} is a n -dimensional vector with all entries equal to 0, except for the j th entry which is equal to 1. Then the full conditional for our model can be written as

$$\begin{aligned} \omega_{ij} | \boldsymbol{\alpha}, \boldsymbol{\beta} &\sim PG(1, \alpha_i + \mathbf{x}_{ij}^\top \boldsymbol{\beta}), \\ \boldsymbol{\alpha} | \mathbf{y}, \boldsymbol{\beta}, \boldsymbol{\omega}, \tau_\alpha^2 &\sim \mathcal{N}(\mathbf{V}_\alpha (\mathbf{Z}^\top \boldsymbol{\Omega} (\tilde{\mathbf{y}} - \mathbf{X} \boldsymbol{\beta}) + \tau_\alpha^{-2} \boldsymbol{\Sigma}_\alpha^{-1} \mathbf{1} \alpha_0), \mathbf{V}_\alpha^{-1}), \\ \boldsymbol{\beta} | \mathbf{y}, \boldsymbol{\alpha}, \boldsymbol{\omega}, \tau_\beta^2 &\sim \mathcal{N}(\mathbf{V}_\beta (\mathbf{X}^\top \boldsymbol{\Omega} (\tilde{\mathbf{y}} - \mathbf{Z} \boldsymbol{\alpha}) + \tau_\beta^{-2} \mathbf{b}_0), \mathbf{V}_\beta^{-1}), \end{aligned}$$

where \mathbf{Z} is the $N \times n$ matrix of \mathbf{z}_{ij} , $\mathbf{V}_\alpha = \mathbf{Z}^\top \boldsymbol{\Omega} \mathbf{Z} + \tau_\alpha^{-2} \boldsymbol{\Sigma}_\alpha^{-1}$, $\mathbf{V}_\beta = \mathbf{X}^\top \boldsymbol{\Omega} \mathbf{X} + \tau_\beta^{-2} \mathbf{I}$. Moreover, $\boldsymbol{\Sigma}_\alpha^{-1}$ denotes the prior covariance matrix of $\boldsymbol{\alpha}$, which is equal to $\boldsymbol{\Sigma}_{\text{CAR}}^{-1}$ under model (3.4) and to \mathbf{I}_n under model (3.11).

Under the CAR prior for $\boldsymbol{\alpha}$, we also need to sample the correlation parameter ρ . Note that this parameter affects the precision matrix of $\boldsymbol{\alpha}$, and its conditional distribution is given by

$$p(\rho | e.e.) = p(\rho | \boldsymbol{\alpha}, \alpha_0, \tau_\alpha^2) \propto |\boldsymbol{\Sigma}_\alpha^{-1}(\rho)|^{1/2} \exp\left(-\frac{1}{2\tau_\alpha^2} (\boldsymbol{\alpha} - \alpha_0 \mathbf{1})^\top \boldsymbol{\Sigma}_\alpha^{-1}(\rho) (\boldsymbol{\alpha} - \alpha_0 \mathbf{1})\right).$$

We sample from this distribution using a Metropolis Hastings-within Gibbs-step, with proposal density $g(\rho^* | \rho_t) = \text{Beta}(\xi \cdot \rho_t / (1 - \rho_t), \xi)$. This ensures that the mean is equal to ρ_t , and we choose $\xi = 5$ so that $g(\rho^* | \rho_t)$ has small variance.

Assuming a half-Cauchy prior on τ_α and on τ_β , i.e. $p(\tau_\alpha) \propto (\tau_\alpha^2 + s_\alpha^2)^{-1}$ and $p(\tau_\beta) \propto (\tau_\beta^2 + s_\beta^2)^{-1}$, their conditional posterior distributions can be written as follows:

$$\begin{aligned} p(\tau_\alpha | \boldsymbol{\alpha}, \alpha_0) &\propto (\tau_\alpha^2 + s_\alpha^2)^{-1} \tau_\alpha^n \exp\left(-\frac{1}{\tau_\alpha^2} (\boldsymbol{\alpha} - \alpha_0 \mathbf{1})^\top \boldsymbol{\Sigma}_\alpha^{-1} (\boldsymbol{\alpha} - \alpha_0 \mathbf{1})/2\right), \\ p(\tau_\beta | \boldsymbol{\beta}, \beta_0) &\propto (\tau_\beta^2 + s_\beta^2)^{-1} \tau_\beta^p \exp\left(-\frac{1}{\tau_\beta^2} \sum_{k=1}^p (\beta_k - b_{0,k})^2/2\right). \end{aligned}$$

To sample from these posterior distributions, we use a Metropolis-Hastings step, with a carefully designed proposal distribution. In general, given a random variable distributed according to $p(x) \propto (x^2 + s^2)^{-1} x^{-2\alpha} \exp(-\beta/x^2)$, consider the following proposal distribution, $q(x) = x^{-2\alpha-1} \exp(-\beta/x^2)$; note that $x \sim q$ is equivalent to $x^2 \sim IG(\alpha, \beta)$. Moreover, if α and β are carefully chosen, the acceptance ratio for the MH steps simplifies considerably:

$$a(x \rightarrow \tilde{x}) = \frac{(x^2 + s^2) \tilde{x}}{(\tilde{x}^2 + s^2) x}.$$

Thus, to sample τ_α from its posterior, we simply need to generate from an inverse gamma distribution with parameters $\alpha = n/2$ and $\beta = (\boldsymbol{\alpha} - \alpha_0 \mathbf{1})^\top \boldsymbol{\Sigma}_\alpha^{-1} (\boldsymbol{\alpha} - \alpha_0 \mathbf{1})/2$, consider its square root as proposed value and compute the acceptance $a(\tau_\alpha \rightarrow \tilde{\tau}_\alpha)$. Similarly, for τ_β we follow the same steps using $\alpha = p/2$ and $\beta = \sum_{k=1}^p (\beta_k - b_{0,k})^2/2$.

Moreover, the full conditional for the remaining parameters are standard:

$$\begin{aligned} \alpha_0 | \boldsymbol{\alpha}, \tau_\alpha^2 &\sim \mathcal{N} \left(\frac{\sum_{i=1}^n \alpha_i / \tau_\alpha^2}{1/\tau_\alpha^2 + 1/100}, \frac{1}{1/\tau_\alpha^2 + 1/100} \right), \\ \mathbf{b}_0 | \boldsymbol{\beta}, \tau_\beta^2 &\sim \mathcal{N} \left(\frac{\boldsymbol{\beta} / \tau_\beta^2}{1/\tau_\beta^2 + 1/100}, \frac{1}{1/\tau_\beta^2 + 1/100} \mathbf{I}_p \right). \end{aligned}$$

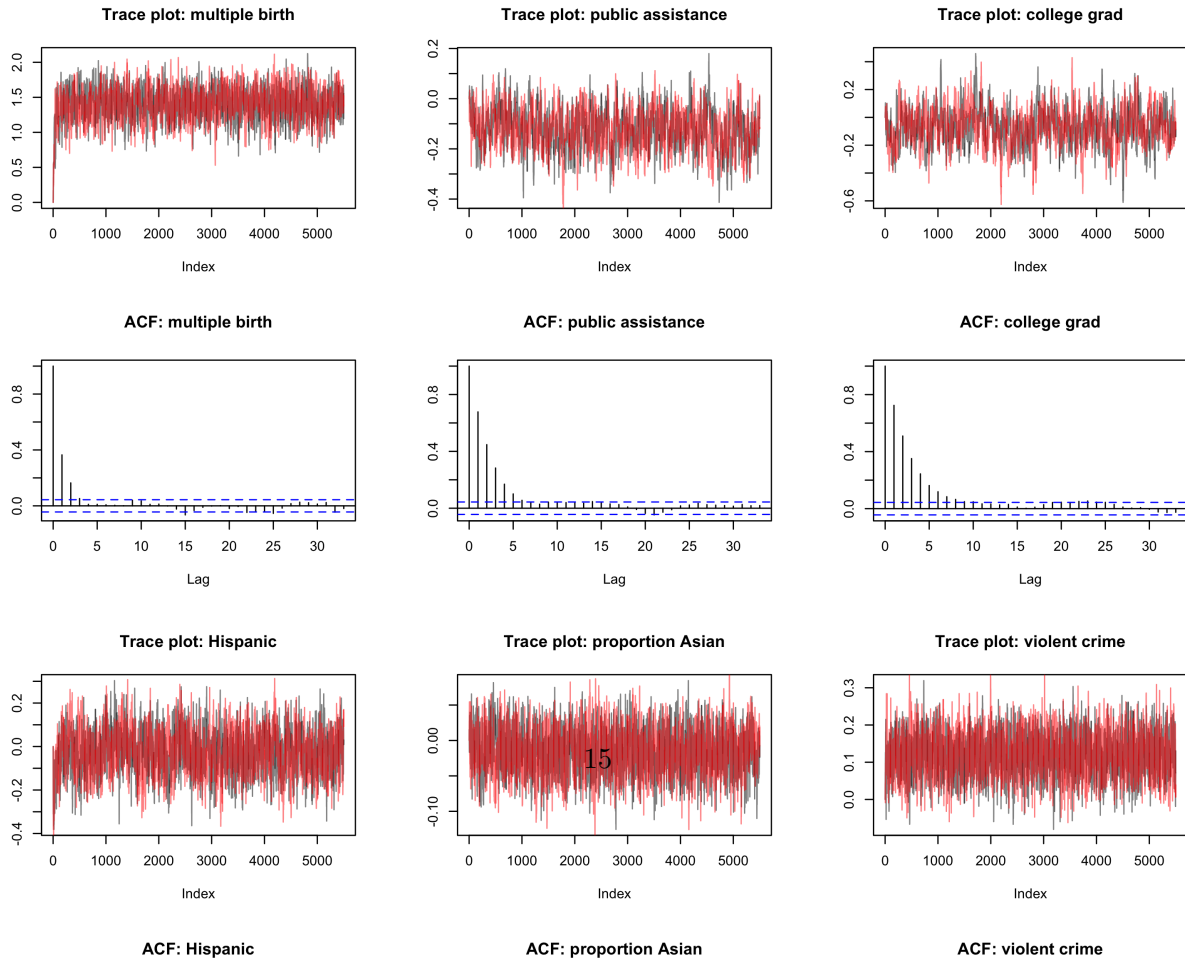
S5.2 MCMC diagnostics

In this section, we report the diagnostics for the MCMC algorithm described in Section S5.1 after we fit the CAR model to the Philadelphia dataset. Table S8 shows the effective sample size (ESS), posterior mean and Monte Carlo standard error (MCSE) for the regression coefficients (i.e. log-odds ratio) of the individual and neighborhood covariates. Results are reported in Table S8 for stillbirth and preterm birth.

Figure S4 shows the trace plots and autocorrelation plots of the MCMC samples for several of the regression coefficients under our CAR model. Figure S4 shows that the MCMC algorithm described in Section S5.1 converged within 5500 iterations for the data that we analyzed in Section 5 of the main manuscript. Moreover, by thinning the chain every 10 iterations, our final MCMC samples were not overly correlated.

	Stillbirth			Preterm birth		
	ESS	β_j	MCSE	ESS	β_j	MCSE
Hispanic	168.2	-0.024	0.0239	662.0	0.449	0.0040
Black	68.3	0.450	0.0238	231.9	0.630	0.0060
Asian	190.3	0.131	0.0342	1011.8	-0.354	0.0047
multiple birth	943.7	2.356	0.0100	4241.4	1.408	0.0014
age	468.4	0.020	0.0035	2511.8	0.029	0.0006
proportion Asian	326.4	-0.016	0.0060	1609.8	-0.026	0.0011
proportion Hispanic	379.6	-0.053	0.0056	1839.4	-0.068	0.0011
proportion Black	293.8	-0.035	0.0111	1183.4	-0.061	0.0020
proportion women	386.6	0.038	0.0050	2064.8	-0.105	0.0008
poverty	450.3	-0.017	0.0059	2462.0	0.243	0.0010
public assistance	430.3	-0.003	0.0050	2249.7	-0.124	0.0008
labor force	399.5	-0.059	0.0062	2042.1	-0.050	0.0010
recent birth	461.4	0.017	0.0037	2230.2	0.038	0.0006
high school grad	432.0	0.109	0.0062	2212.4	0.068	0.0010
college grad	356.7	-0.074	0.0090	1780.7	-0.068	0.0015
occupied housing	377.2	-0.015	0.0054	1821.4	0.063	0.0009
housing violation	416.0	-0.033	0.0058	1869.5	-0.099	0.0011
violent crime	413.7	0.120	0.0097	1881.7	0.166	0.0017
nonviolent crime	375.0	-0.027	0.0064	1836.8	-0.086	0.0011

Table S8: Effective sample size (ESS), posterior mean regression coefficient (β_j), and Monte Carlo standard error (MCSE) for β_j under the CAR model. These diagnostics are reported for both stillbirth and preterm birth.



References

- [1] Albert, J. H. and S. Chib (1993). Bayesian analysis of binary and polychotomous response data. Journal of the American Statistical Association 88(422), 669–679.
- [2] Balocchi, C. and S. T. Jensen (2019). Spatial modeling of trends in crime over time in Philadelphia. The Annals of Applied Statistics 13(4), 2235–2259.
- [3] Banerjee, S., B. Carlin, and A. Gelfand (2014). Hierarchical Modeling and Analysis for Spatial Data, Second Edition. Chapman & Hall/CRC Monographs on Statistics & Applied Probability. Taylor & Francis.
- [4] Besag, J. (1974). Spatial interaction and the statistical analysis of lattice systems. Journal of the Royal Statistical Society: Series B (Statistical Methodology) 36(2), 192–225.
- [5] Bivand, R. and N. Lewin-Koh (2019). maptools: Tools for Handling Spatial Objects. R package version 0.9-9.
- [6] Bivand, R. and D. W. S. Wong (2018). Comparing implementations of global and local indicators of spatial association. TEST 27(3), 716–748.
- [7] Boland, M. R., J. Liu, C. Balocchi, J. Meeker, R. Bai, I. Mellis, D. L. Mowery, and D. Herman (2021). Association of neighborhood-level factors and COVID-19 infection patterns in philadelphia using spatial regression. AMIA Joint Summits on Translational Science proceedings. AMIA Joint Summits on Translational Science, 2021, 545–554.
- [8] Canelón, S. P., H. H. Burris, L. D. Levine, and M. R. Boland (2021). Development and evaluation of MADDIE: Method to acquire delivery date information from electronic health records. International Journal of Medical Informatics 145, 104339.
- [9] Chawla, N. V., K. W. Bowyer, L. O. Hall, and W. P. Kegelmeyer (2002). SMOTE: Synthetic minority over-sampling technique. Journal of Artificial Intelligence Research 16(1), 321–357.
- [10] Chen, C., A. Liaw, and L. Breiman (2004). Using random forest to learn imbalanced data. Technical report.
- [11] Dahl, D. B., D. Scott, C. Roosen, A. Magnusson, and J. Swinton (2019). xtable: Export Tables to LaTeX or HTML. R package version 1.8-4.
- [12] Dankwa-Mullan, I. and E. J. Pérez-Stable (2016). Addressing health disparities is a place-based issue. American Journal of Public Health 106(4), 637–639.
- [13] Dekker, G. A., S. Y. Lee, R. A. North, L. M. McCowan, N. A. B. Simpson, and C. T. Roberts (2012). Risk factors for preterm birth in an international prospective cohort of nulliparous women. PLOS ONE 7(7), 1–9.
- [14] Ferré, C., W. Callaghan, C. Olson, A. Sharma, and W. Barfield (2016). Effects of maternal age and age-specific preterm birth rates on overall preterm birth rates — United States, 2007 and 2014. MMWR Morbidity and Mortality Weekly Report 65(43), 1181–1184.

- [15] Gelman, A., J. Hwang, and A. Vehtari (2014). Understanding predictive information criteria for bayesian models. Statistics and computing 24(6), 997–1016.
- [16] Genz, A., F. Bretz, T. Miwa, X. Mi, F. Leisch, F. Scheipl, and T. Hothorn (2020). mvtnorm: Multivariate Normal and t Distributions. R package version 1.1-0.
- [17] Goldenberg, R. L., J. F. Culhane, J. D. Iams, and R. Romero (2008). Epidemiology and causes of preterm birth. The Lancet 371(9606), 75–84.
- [18] He, J. and M. X. Cheng (2021). Weighting methods for rare event identification from imbalanced datasets. Frontiers in Big Data 4.
- [19] Jardine, J., K. Walker, I. Gurol-Urganci, K. Webster, P. Muller, J. Hawdon, A. Khalil, T. Harris, J. van der Meulen, N. Maternity, et al. (2021). Adverse pregnancy outcomes attributable to socioeconomic and ethnic inequalities in england: a national cohort study. The Lancet 398(10314), 1905–1912.
- [20] Kahle, D. and H. Wickham (2013). ggmap: Spatial visualization with ggplot2. The R Journal 5(1), 144–161.
- [21] King, G. and L. Zeng (2001, Spring). Logistic regression in rare events data. Political Analysis 9, 137–163.
- [22] Kramer, M. R., H. L. Cooper, C. D. Drews-Botsch, L. A. Waller, and C. R. Hogue (2010). Metropolitan isolation segregation and black–white disparities in very preterm birth: A test of mediating pathways and variance explained. Social Science and Medicine 71(12), 2108 – 2116.
- [23] Kramer, M. R. and C. R. Hogue (2008). Place matters: Variation in the black/white very preterm birth rate across U.S. metropolitan areas, 2002–2004. Public Health Reports 123(5), 576–585. PMID: 18828412.
- [24] Kramer, M. S. (2003). The epidemiology of adverse pregnancy outcomes: An overview. The Journal of Nutrition 133(5), 1592S–1596S.
- [25] Kuhn, M. and K. Johnson (2013). Applied Predictive Modeling. Springer.
- [26] Lee, D. (2011). A comparison of conditional autoregressive models used in Bayesian disease mapping. Spatial and Spatio-temporal Epidemiology 2(2), 79–89.
- [27] Leroux, B. G., X. Lei, and N. Breslow (2000). Estimation of disease rates in small areas: A new mixed model for spatial dependence. In M. E. Halloran and D. Berry (Eds.), Statistical Models in Epidemiology, the Environment, and Clinical Trials, New York, NY, pp. 179–191. Springer New York.
- [28] Macdorman, M. F. and E. C. W. Gregory (2015). Fetal and perinatal mortality: United states, 2013. National Vital Statistics Reports 64(8), 1–24.
- [29] Makowski, D., M. S. Ben-Shachar, S. Chen, and D. Lüdtke (2019). Indices of effect existence and significance in the bayesian framework. Frontiers in Psychology 10, 2767.

- [30] Mandujano, A., T. P. Waters, and S. A. Myers (2013). The risk of fetal death: current concepts of best gestational age for delivery. American Journal of Obstetrics and Gynecology 208(3), 207.e1 – 207.e8.
- [31] Manski, C. and S. R. Lerman (1977). The estimation of choice probabilities from choice based samples. Econometrica 45(8), 1977–88.
- [32] Martin, J., B. Hamilton, M. Osterman, A. Driscoll, P. Drake, and National Center for Health Statistics (U.S.) (2018). Births: Final data for 2017. National Vital Statistics Reports 67(8).
- [33] Masi, C. M., L. C. Hawkley, Z. H. Piotrowski, and K. E. Pickett (2007). Neighborhood economic disadvantage, violent crime, group density, and pregnancy outcomes in a diverse, urban population. Social Science & Medicine 65(12), 2440–2457.
- [34] Mattison, D. R., K. Damus, E. Fiore, J. Petrini, and C. Alter (2001). Preterm delivery: a public health perspective. Paediatric and Perinatal Epidemiology 15(s2), 7–16.
- [35] Mayne, S. L., L. R. Pool, W. A. Grobman, and K. N. Kershaw (2018). Associations of neighbourhood crime with adverse pregnancy outcomes among women in Chicago: analysis of electronic health records from 2009 to 2013. Journal of Epidemiology and Community Health 72(3), 230–236.
- [36] McGowan, V. J., S. Buckner, R. Mead, E. McGill, S. Ronzi, B. F., and C. Bamba (2021). Examining the effectiveness of place-based interventions to improve public health and reduce health inequalities: an umbrella review. BMC Public Health 21, 1888.
- [37] Meeker, J. R., S. P. Canelón, R. Bai, L. Levine, and M. R. Boland (2021). Individual-level and neighborhood-level risk factors for severe maternal morbidity. Obstetrics & Gynecology, to appear.
- [38] Meghea, C. I. and W. Corser (2016). Electronic medical record use and maternal and child care and health. Maternal and Child Health Journal 20, 819–826.
- [39] Moran, P. A. P. (1950). Notes on continuous stochastic phenomena. Biometrika 37(1/2), 17–23.
- [40] Muraskas, J. and K. Parsi (2008). BART with targeted smoothing: An analysis of patient-specific stillbirth risk. AMA Journal of Ethics 10(10), 655–658.
- [41] Neter, J., M. H. Kutner, C. J. Nachtsheim, and W. Wasserman (2004). Applied Linear Statistical Models (4th ed.). McGraw-Hill Irwin.
- [42] Pebesma, E. J. and R. S. Bivand (2005, November). Classes and methods for spatial data in R. R News 5(2), 9–13.
- [43] Polson, N. G., J. G. Scott, and J. Windle (2013). Bayesian inference for logistic models using Pólya–Gamma latent variables. Journal of the American Statistical Association 108(504), 1339–1349.
- [44] R Core Team (2020). R: A Language and Environment for Statistical Computing. Vienna, Austria: R Foundation for Statistical Computing.

- [45] Robin, X., N. Turck, A. Hainard, N. Tiberti, F. Lisacek, J.-C. Sanchez, and M. Müller (2011). pROC: an open-source package for R and S+ to analyze and compare ROC curves. BMC Bioinformatics 12, 77.
- [46] Santafe, G., B. Calvo, A. Perez, and J. A. Lozano (2022). bde: Bounded Density Estimation. R package version 1.0.1.1.
- [47] Shapiro-Mendoza, C. K., W. D. Barfield, Z. Henderson, A. James, J. L. Howse, J. Iskander, and P. G. Thorpe (2016). CDC grand rounds: Public health strategies to prevent preterm birth. MMWR Morbidity and Mortality Weekly Report 65(32), 826–830.
- [48] Sharpe, E. K. (2013). Targeted neighbourhood social policy: a critical analysis. Journal of Policy Research in Tourism, Leisure and Events 5(2), 158–171.
- [49] South, A. P., D. E. Jones, E. S. Hall, S. Huo, J. Meinzen-Derr, L. Liu, and J. M. Greenberg (2012). Spatial analysis of preterm birth demonstrates opportunities for targeted intervention. Maternal and Child Health Journal 16, 470–478.
- [50] Spiegelhalter, D. J., N. G. Best, B. P. Carlin, and A. Van Der Linde (2002). Bayesian measures of model complexity and fit. Journal of the Royal Statistical Society: Series B (Statistical Methodology) 64(4), 583–639.
- [51] Starling, J. E., J. S. Murray, C. M. Carvalho, R. K. Bukowski, and J. G. Scott (2020). BART with targeted smoothing: An analysis of patient-specific stillbirth risk. The Annals of Applied Statistics 14(1), 28–50.
- [52] Statisticat and LLC. (2021). LaplacesDemon: Complete Environment for Bayesian Inference. R package version 16.1.6.
- [53] Torgo, L. (2013). DMWR: Functions and data for “Data Mining with R”. R package version 0.4.1.
- [54] Torgo, L. (2014). An infra-structure for performance estimation and experimental comparison of predictive models in r. CoRR abs/1412.0436.
- [55] Warren, J., M. Fuentes, A. Herring, and P. Langlois (2012). Spatial-temporal modeling of the association between air pollution exposure and preterm birth: Identifying critical windows of exposure. Biometrics 68(4), 1157–1167.
- [56] Watanabe, S. and M. Opper (2010). Asymptotic equivalence of Bayes cross validation and widely applicable information criterion in singular learning theory. Journal of Machine Learning Research 11(12), 3571–3594.
- [57] Wickham, H. (2016). ggplot2: Elegant Graphics for Data Analysis. Springer-Verlag New York.
- [58] Wickham, H., R. François, L. Henry, and K. Müller (2020). dplyr: A Grammar of Data Manipulation. R package version 0.8.5.
- [59] Xu, J., S. L. Murphy, K. D. Kochanek, and B. A. Bastian (2016). Deaths: Final data for 2013. National Vital Statistics Reports 10(10), 1–119.

- [60] Zahrieh, D., J. J. Oleson, and P. A. Romitti (2019a). Bayesian point process modeling to quantify geographic regions of excess stillbirth risk. Geographical Analysis 51(3), 381–400.
- [61] Zahrieh, D., J. J. Oleson, and P. A. Romitti (2019b). Quantifying geographic regions of excess stillbirth risk in the presence of spatial and spatio-temporal heterogeneity. Spatial and Spatio-temporal Epidemiology 29, 97–109.
- [62] Zhao, Y., Z. S.-Y. Wong, and K. L. Tsui (2018). A framework of rebalancing imbalanced healthcare data for rare events’ classification: A case of look-alike sound-alike mix-up incident detection. Journal of Healthcare Engineering 2018, Article ID 6275435.